



Review

A review of ocean color remote sensing methods and statistical techniques for the detection, mapping and analysis of phytoplankton blooms in coastal and open oceans



David Blondeau-Patissier ^{a,*}, James F.R. Gower ^b, Arnold G. Dekker ^{c,d}, Stuart R. Phinn ^d, Vittorio E. Brando ^{c,d}

^a North Australian Marine Research Alliance (NAMRA), The Research Institute for the Environment and Livelihoods (RIEL), Charles Darwin University, Darwin, Australia

^b Fisheries and Oceans Canada, Institute of Ocean Sciences, Sidney, Canada

^c CSIRO Land and Water, Aquatic Remote Sensing Group, Canberra, Australia

^d School of Geography, Planning and Environmental Management, The University of Queensland, Brisbane, Australia

ARTICLE INFO

Article history:

Received 26 June 2013

Received in revised form 27 December 2013

Accepted 31 December 2013

Available online 27 January 2014

ABSTRACT

The need for more effective environmental monitoring of the open and coastal ocean has recently led to notable advances in satellite ocean color technology and algorithm research. Satellite ocean color sensors' data are widely used for the detection, mapping and monitoring of phytoplankton blooms because earth observation provides a synoptic view of the ocean, both spatially and temporally. Algal blooms are indicators of marine ecosystem health; thus, their monitoring is a key component of effective management of coastal and oceanic resources. Since the late 1970s, a wide variety of operational ocean color satellite sensors and algorithms have been developed. The comprehensive review presented in this article captures the details of the progress and discusses the advantages and limitations of the algorithms used with the multi-spectral ocean color sensors CZCS, SeaWiFS, MODIS and MERIS. Present challenges include overcoming the severe limitation of these algorithms in coastal waters and refining detection limits in various oceanic and coastal environments. To understand the spatio-temporal patterns of algal blooms and their triggering factors, it is essential to consider the possible effects of environmental parameters, such as water temperature, turbidity, solar radiation and bathymetry. Hence, this review will also discuss the use of statistical techniques and additional datasets derived from ecosystem models or other satellite sensors to characterize further the factors triggering or limiting the development of algal blooms in coastal and open ocean waters.

Crown Copyright © 2014 Published by Elsevier Ltd. This is an open access article under the CC BY-NC-SA license (<http://creativecommons.org/licenses/by-nc-sa/3.0/>).

Contents

1. Introduction	124
2. Algal blooms in the context of this review.....	125
3. Ocean color remote sensing algorithms	126
3.1. Reflectance classification algorithms	126
3.2. Reflectance band-ratio algorithms	127
3.2.1. Blue-green band-ratios for open and coastal ocean waters	128
3.2.2. The relevance of the red-NIR spectral regions in coastal waters.....	130

Abbreviations: AVHRR, Advanced Very High Resolution Radiometer; Chl-i, Chlorophyll concentration of pigment i; CDOM, Colored Dissolved Organic Matter; CIA, Color Index Algorithm; CZCS, Coastal Zone Color Scanner (NASA); EMD, Empirical Mode Decomposition; EOF, Empirical Orthogonal Function; FAI, Floating Algae Index; FLH, Fluorescence Line Height; GSM, Garver-Siegel-Maritorena model; HAB, Harmful Algal Bloom; HNLC, High Nutrient-Low Chlorophyll; HPLC, High Performance Liquid Chromatography; KBBI, Karenia brevis Bloom index; MCI, Maximum Chlorophyll Index; MERIS, Medium Resolution Imaging Spectrometer (ESA); MODIS, Moderate Resolution Imaging Spectroradiometer (NASA); NIR, Near Infrared (>700 nm); PAR, Photosynthetically Active Radiation; PCA, Principal Component Analysis; QAA, Quasi-Analytical Algorithm; RBD, Red Band Difference; RCA, Red tide index Chlorophyll Algorithm; RGB, Red-Green-Blue true color satellite image; RI, Red Tide Index; Rrs, Remote Sensing Reflectance; SeaWiFS, Sea-viewing Wide Field-of-view Sensor (NASA); SSH, Sea Surface Height; SST, Sea Surface Temperature; TSM, Total Suspended Matter.

* Corresponding author. Tel.: +61 0 8 8946 6646.

E-mail address: David.Blondeau-Patissier@cdu.edu.au (D. Blondeau-Patissier).

3.2.3. Band-ratio algorithms: Limitations and challenges	130
3.3. Spectral band difference algorithms	131
3.3.1. Fluorescence Line Height (FLH)	131
3.3.2. Maximum Chlorophyll Index (MCI)	132
3.3.3. Floating Algae Index (FAI) and Scaled Algae Index (SAI)	132
3.3.4. Color Index Algorithm (CIA)	132
3.3.5. Spectral band difference algorithms: Limitations and challenges	132
3.4. Bio-optical models	132
3.4.1. Retrieval of taxa-specific pigment concentrations from bio-optical models	133
3.4.2. Derivation of inherent optical properties from bio-optical models for the detection of algal blooms	133
3.4.3. Bio-optical models: Limitations and challenges	133
4. The detection of specific types of algal blooms	133
4.1. Algal blooms with surface expressions	133
4.1.1. Coccolithophore blooms	133
4.1.2. Trichodesmium blooms	133
4.1.3. Floating Sargassum	134
4.1.4. Harmful Algal blooms – Example of dinoflagellate <i>Karenia brevis</i>	134
5. Statistical techniques and data assimilation to assess phytoplankton bloom dynamics	134
5.1. Statistical partitioning of marine ecosystems	134
5.2. Time-series, fitted models and signal processing techniques	135
5.3. Satellite product climatologies and merging data from multiple sources	138
6. Conclusions and future directions	138
Acknowledgments	139
References	139

1. Introduction

Over 5000 species of marine phytoplankton have been described worldwide (e.g., [Sournia et al., 1991](#)). Typically ranging from less than 1 µm to over 100 µm in size, a phytoplankton cell, also known as an ‘algal’ or ‘algae’ cell, is a planktonic photosynthesizing organism. Increases in phytoplankton cell numbers can result from favorable environmental conditions, which include water column stratification, increase in light availability (e.g., [Gohin et al., 2003](#); [Kogeler and Rey, 1999](#)), water temperature ([Thomas et al., 2003](#)) and/or nutrient levels (e.g., [Santolieri et al., 2003](#); [Siegel et al., 1999](#)). The global distribution of Chlorophyll-a (Chl-a), the direct proxy for phytoplankton biomass ([Cullen, 1982](#)), shows that Chl-a-rich regions are located along the coasts and continental shelves, north of 45° North ([Fig. 1a](#)), mostly because of a strong nutrient supply. Moderate Chl-a concentrations are found in the equatorial regions of the Atlantic and Pacific, caused by the upwelling of deep, nutrient-rich, cool waters from the divergence of the ocean water masses along the equator. Moderate Chl-a concentrations are also found in the subtropical convergence zone (south of 45° South), where cool, nutrient-rich sub-Antarctic water masses mix with warm, nutrient-poor subtropical waters. However, most open ocean regions typically appear low in satellite-derived Chl because they are far from land. Ocean color observations are limited to the first optical depth; consequently, deep chlorophyll maxima (DCM) are not always captured by satellites (e.g., [Huisman et al., 2006](#); [Cullen, 1982](#)). Many phytoplankton blooms (see Section 2) occurring deep in the water column or with extremely low Chl-a (<0.1 mg m⁻³) remain unreported because they are not always observed in satellite images but yet are known to occur (e.g., [Dore et al., 2008](#); [Villareal et al., 2011](#)). Algal blooms (see Section 2) detected by satellite sensors often cover large areas, but their typically “patchy” distributions make them difficult to model ([Martin, 2003](#)) ([Fig. 1b-d](#)). The visualization of satellite images ([Fig. 1](#)) is the primary technique used to identify their presence, particularly when phytoplankton blooms occur as a regular event in a specific ocean region (e.g., [Srokosz and Quartly, 2013](#)) or in regions where they are not usually expected, such as oligotrophic gyres (e.g., [Wilson, 2003](#); [Wilson et al., 2008](#); [Wilson and Qiu, 2008](#)). Over the last 13 years, there has been an increase in peer-reviewed publications

on the study of algal blooms using ocean color satellite data ([Fig. 2](#)). Algal blooms in coastal ocean regions have been the primary focus of those studies, mainly due to the direct connectivity between the land and continental shelf waters (e.g., [Gazeau et al., 2004](#)) and the impact of coastal harmful phytoplankton blooms on anthropogenic activities ([Frolov et al., 2013](#)). Important technological progress in the design of satellite ocean color sensors from the second and third generations greatly improved coastal water algorithms, resulting in a more accurate retrieval of phytoplankton proxies in coastal waters (see Table 1 of [Shen et al. \(2012\)](#); [Fig. 3](#)).

Phytoplankton blooms affect the color of the water by increasing light backscattering with spectrally localized water-leaving radiance minima from generic (Chl-a) and species-specific algal pigment absorption, such as phycobiliproteins for cyanobacteria, fucoxanthin for diatoms and peridinin for dinoflagellates. Ocean color remote sensing, the passive satellite-based measurement of visible light emerging from the ocean surface ([Robinson, 2004](#)), has provided more than two decades of near-real-time synoptic and recurrent measurements of global phytoplankton biomass ([Figs. 1 and 4](#)), evolving from qualitative (e.g., [Gordon et al., 1980](#)) to quantitative estimates (e.g., [Kutser, 2009](#)). The accumulation of scientific knowledge on the temporal and spatial dynamics of phytoplankton in the world’s oceans from earth observations was largely assisted by rapid advances in marine science technologies (e.g., [Babin et al., 2008](#); [Dickey et al., 2006](#)) and has had many global and local applications ([Table 1](#)). Recent reviews on satellite ocean color remote sensing have reported on, but are not limited to, scientific advances in this field (e.g., [McClain, 2009a, 2009b](#)), its societal benefits (e.g., [IOC/CC Report 7, 2008](#)) and its valuable applications to coastal ecosystem management (e.g., [Kratzer et al., 2013](#); [Klemas, 2011](#)), including that of fisheries (e.g., [Wilson, 2011](#)) and in the detection of (harmful) algal blooms ([Shen et al., 2012](#)) ([Table 2](#)).

The reviews of [Matthews \(2011\)](#) and [Odermatt et al. \(2012\)](#) discussed the various ocean color models used for the retrieval of water quality parameters in open and coastal ocean waters, from empirical to more complex approaches. More recently, [Brody et al. \(2013\)](#) compared different methods to determine phytoplankton bloom initiation. The present article will complement those recent reviews by providing the following:

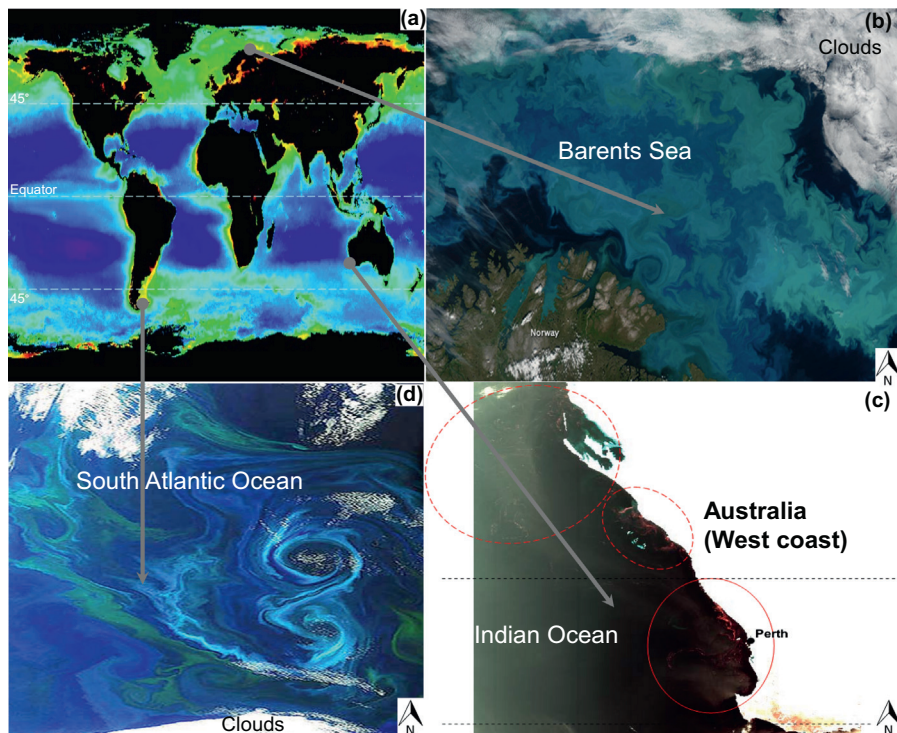


Fig. 1. (a) The global distribution of chlorophyll averaged over the period from 1 January 2002 to 31 January 2008 using data collected from MODIS-Aqua; Chlorophyll values range from 0.01 mg m^{-3} (purple) to 60 mg m^{-3} (red) (NASA/GSFC); (b) NASAMODIS-Aqua captures a coccolithophore bloom in the Barents Sea on August 14, 2011 (credit: NASA); (c) ESAMERIS reduced-resolution RGB-stretched image showing surface bloom expressions (circled in red) off the Australian West coast on March 10, 2009 (from Blondeau-Patissier, 2011); (d) ESAMERIS full-resolution (300 m) true-color image showing a southern hemisphere spring phytoplankton bloom (green swirls) in the South Atlantic Ocean, 600 km east off the Falkland Islands, on December 2, 2011. “The figure-eight pattern in the image is likely to be an example of von Karman vortices, which are formed when an obstacle blocks a prevailing wind or ocean current” (credit: ESA). (For interpretation of the references to colour in this figure legend, the reader is referred to the web version of this article.)

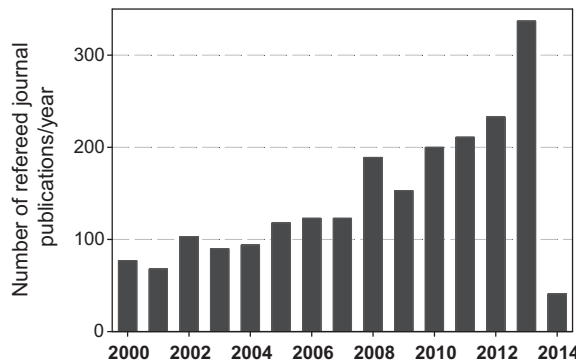


Fig. 2. Number of peer-reviewed journal publications per year since 2000 based on the results of a Boolean search with the terms “ocean color” and “phytoplankton algal bloom” in ScienceDirect® (as of December 16, 2013). Data for the year 2014 refer to accepted publications that are available online and expected to be published between January and February 2014.

1. A comparative analysis of algorithm types specifically used for the detection, mapping and analysis of algal blooms from passive multi-spectral ocean color sensors’ imagery. Advantages and limitations in the application of the techniques presented will be discussed.
2. A synthesis of the ocean color remote sensing methods used for the detection of four specific types of blooms. An exception is made for pelagic *Sargassum*, which are macro-algae and not typically defined as phytoplankton.

3. An examination of the statistical techniques that are often used in combination with an ocean color dataset for the detection and monitoring of algal blooms.

The detection of phytoplankton functional types, phytoplankton size classes and phytoplankton primary production derived from ocean color remote sensing data will not be reviewed in this article. Tables 1–6 classify the peer-reviewed publications published between 2000 and 2014 according to the research application, the ocean color sensor used, the phytoplankton bloom types and the techniques employed to detect those events.

2. Algal blooms in the context of this review

The various definitions of phytoplankton blooms often rely on different, and sometimes arbitrary, criteria, such as the biomass or growth rate, or both. The review article by Kutser (2009) warned in the introduction that the term “bloom” is “relative” because it is used to describe phytoplankton events with contrastingly different biomass concentrations (p. 4402). Richardson (1997) defined an algal bloom as “*the rapid growth of one or more species which leads to an increase in biomass of the species*” (p. 302). In the context of this review, a phytoplankton bloom will be defined as a biological event composed of micro-algal species (see Bricaud et al. (2004) for phytoplankton cell sizes and ranges of Chl-a concentrations) that is sustained both over time and space and that results in noticeable changes in satellite radiances at wavelengths used for algal bloom proxies due to an increase in biomass (in comparison to surrounding algal bloom-free waters).

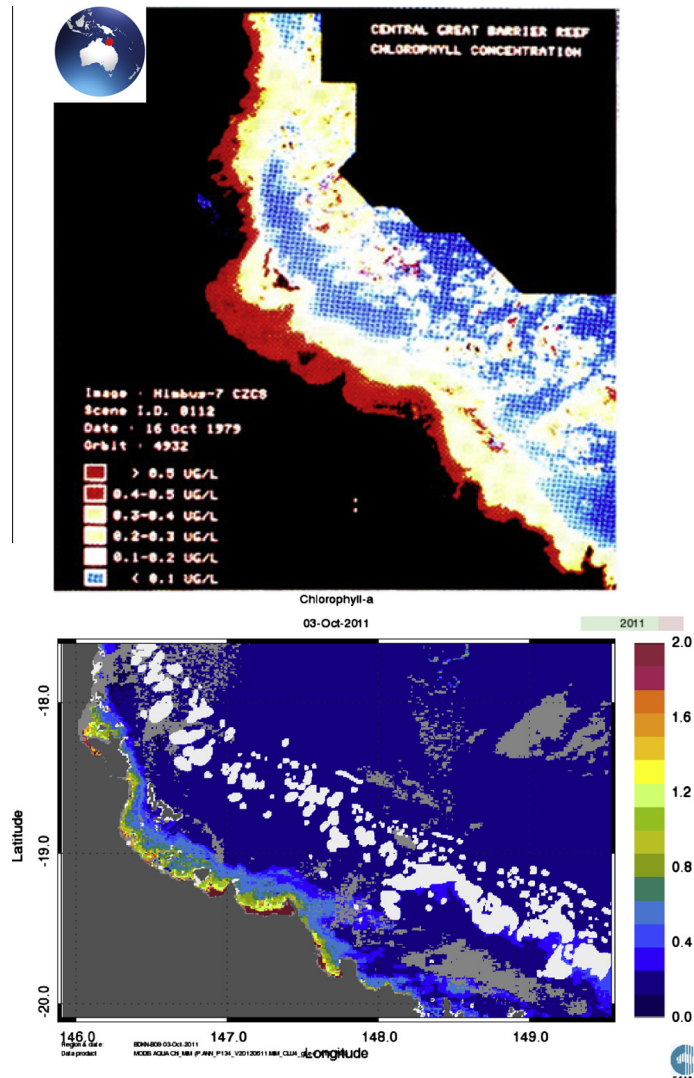


Fig. 3. Examples of Chl-a satellite images from the first and second generations of ocean color sensors. Top panel: a CZCS image on October 16, 1979 from Cairns to Broad Sound, Great Barrier Reef, Australia (Gabric et al., 1990); Bottom panel: the same region as observed from MODIS-Aqua on October 3, 2011. Chl-a was derived using the Matrix Inversion Method (Brando et al., 2012) and SeaDAS 6.4. Clouds and Land are masked in gray and the submerged reef matrix is masked in white. Chl-a is expressed in $\mu\text{g/L}$. (For interpretation of the references to colour in this figure legend, the reader is referred to the web version of this article.)

3. Ocean color remote sensing algorithms

The need for accurate retrievals of Chl concentrations in open and coastal ocean waters from ocean color data has driven most of the research in algorithm development over the past thirty years. Other algorithms have also been developed, such as those that use specific spectral features of the reflectance spectrum to detect phytoplankton with surface expressions. There is a wide variety of operational ocean color satellite sensors and algorithms to assist in the detection and monitoring of phytoplankton blooms, and this section explores the various forms currently available, which specifically includes reflectance-based classification algorithms, spectral band-ratios, spectral band-difference algorithms and bio-optical models. The limitations and advantages associated with their application in the detection and mapping of algal blooms are discussed.

3.1. Reflectance classification algorithms

It has long been recognized that information about optically active constituents present within a parcel of water can be obtained from its spectral reflectance spectrum (e.g., Steemann Nielsen,

1963, 1937; Steemann Nielsen and Jensen, 1957). Spectral bands located in the blue, green, yellow, red or near-infrared (NIR) portion of the reflectance spectrum can be used in many ways to detect algal blooms (Figs. 5 and 6). Algorithms that rely mostly on the detection of specific spectral features are often well suited for algal blooms with surface expressions. This approach can be sufficient for the discrimination of algal blooms from other naturally occurring phenomena (e.g., Siegel et al., 2007), but the sole use of the reflectance spectrum can often only provide qualitative estimates. The reliability of the measured reflectance is hampered by its sensitivity to, e.g., the thickness of the floating algal layer, suspended particulates, bottom reflectance (although novel correction techniques now exist (e.g., Barnes et al., 2013)) and atmospheric correction errors. This reliability is even more questionable when dealing with coastal waters, where other optically active substances affect the water-leaving radiance. To ensure the validity of the algal bloom information retrieved from reflectance classification algorithms, it is recommended that knowledge of the study region be taken into account. A detailed analysis of the reflectance spectra of the flagged pixels is also required. Section 4.1 provides further discussion for the specific detection of Coccolithophore and Trichodesmium blooms.

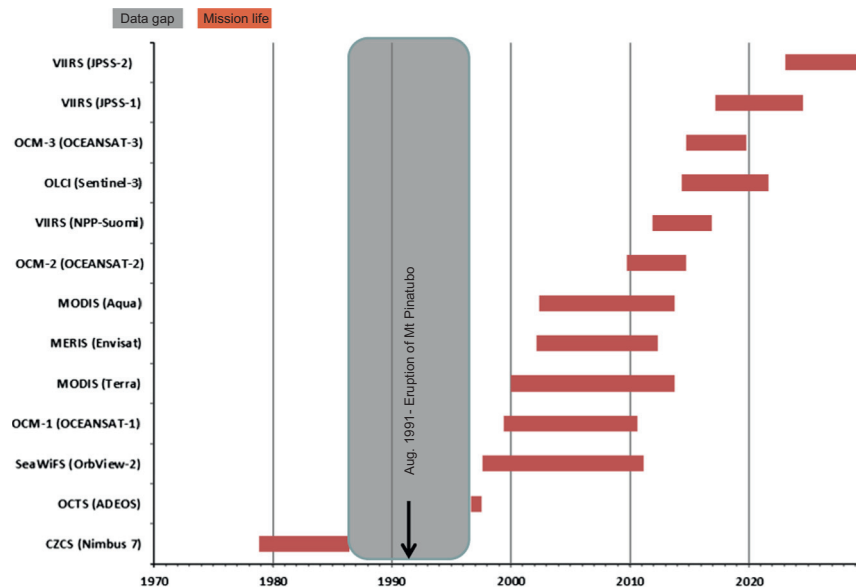


Fig. 4. Timeline 1970–2030 illustrating past, current, and future global ocean-color satellite missions. Missions after 1999 were extracted from the online CEOS Earth Observation Handbook (<http://www.eohandbook.com/>). Satellite platforms are indicated. (For interpretation of the references to colour in this figure legend, the reader is referred to the web version of this article.)

Table 1

Detecting algal blooms from ocean color remote sensing: applications overview (cited research from 2006 to 2013 is indicative only).

Research application	Global scale	Local scale
Spatial and temporal distributions (phenology)	Gower and King (2011a), Gower et al. (2008), Demarcq et al. (2012) and Racault et al. (2012)	Park et al. (2010b), Garcia and Garcia (2008), Gower and King (2007a), Song et al. (2010), Platt and Sathyendranath (2008), Henson et al. (2009)
Derivation of long terms baseline, and marine ecosystem's response to i.e., climatic, anthropogenic forcing	Martinez et al. (2009) and Siegel et al. (2013)	Kahru et al. (2010), Shi and Wang (2007) and Zhao et al. (2008)
Ecosystem partitioning	IOCCG (2009), Oliver and Irwin (2008) and Platt et al. (2008)	Henson et al. (2006)
Coastal zone management (eutrophication, etc.)	Smetacek and Cloern (2008)	Penaflor (2007), Banks et al. (2012), Klemas (2011)
Biogeochemistry (carbon, nitrogen fluxes, etc.)	Platt et al. (2008)	Chang and Xuan (2011) and Focardi et al. (2009)
Major phytoplankton groups (Coccolithophores, <i>Trichodesmium</i> , etc.)	Moore et al. (2012)	Carvalho et al. (2011), Miller et al. (2006), Shutler et al. (2012), McKinna et al. (2011) and Gower and King (2011b)
Size-class, community composition and physiology	Brewin et al. (2011), Behrenfeld et al. (2009) and Gower and King (2011a)	Pan et al. (2012, 2013)
Extremes (e.g., super-blooms)		Gower and King (2007a)

Table 2

Spectral bands (in nm) used in algal bloom indices for SeaWiFS, MODIS and MERIS (cited research is indicative only).

Sensor	Product	Band 1	Band 2	Band 3	Algal bloom type	References
MODIS	FLH	667	678	746	Algal blooms, surface algal blooms	Hu et al. (2005)
MERIS	FLH	665	681	708.75	Algal blooms	Gower et al. (2003)
MODIS	FAI	667	859	1240 or 1640	Surface algal blooms	Hu (2009)
SeaWiFS	CIA	443	555	670	Low Chlorophyll concentrations	Hu et al. (2012)
MERIS	MCI	681	708.75	753	High concentration in water and surface algal blooms	Gower et al. (2003)
MERIS	MCI _{wide}	665	708.75	753	High concentration in water and surface algal blooms	Gower et al. (2004)
MERIS	EBI	665	708.75	n/a	Surface algal blooms	(Not peer-reviewed) Amin, R. Ahn and Shanmugam (2006)
SeaWiFS	RI	443	510	555	Algal blooms	Ahn and Shanmugam (2006)
SeaWiFS	ABI	443	490	555	HAB, algal blooms	Shanmugam (2011) and Ahn and Shanmugam (2006)
MODIS	ABI	443	490	555	HAB, algal blooms	Shanmugam (2011) and Ahn and Shanmugam (2006)
MODIS	KBBI & RBD	667	678	n/a	Surface algal blooms (<i>K. brevis</i>)	Amin et al. (2009b)
MERIS	KBBI & RBD	665	681	n/a	Surface algal blooms (<i>K. brevis</i>)	Amin et al. (2008)

Table 3

Detecting phytoplankton blooms with CZCS (cited research is indicative only).

Phytoplankton type	Reflectance classification (thresholds, anomalies)	Reflectance band-ratios	Bio-optical model or neural network	Spectral band difference	Satellite product (threshold or anomaly) and climatology, statistics
Phytoplankton bloom (undefined)		Banse and English (2000), Kim et al. (2000), Yoder et al. (2001), Shevyrnogov et al. (2002b), Robinson et al. (2004) and Tang et al. (2004)			Banse and English (1999), Shevyrnogov et al. (2002a), Marinelli et al. (2008) and Antoine et al. (2005) ^a
Surface expression (undefined)					
Coccolithophores	Merico et al. (2003)				
Trichodesmium					
Red tides/HAB					

^a Merged with SeaWiFS.**Table 4**

Detecting phytoplankton blooms with SeaWiFS (cited research is indicative only).

Phytoplankton type	Reflectance classification (thresholds, anomalies)	Reflectance band-ratios	Bio-optical model or neural network	Spectral band difference	Satellite product (threshold or anomaly) and climatology, statistics
Phytoplankton bloom (undefined)	Otero and Siegel (2004)	Gower (2001), Lavender and Groom (2001), Gohin et al. (2003), Santoleri et al. (2003), Thomas et al. (2003), Vinayachandran and Mathew (2003), Claustre and Maritorena (2003), Babin et al. (2004), Otero and Siegel (2004), Ahn et al. (2005), Iida and Saitoh (2007) and Siegel et al. (2013)	Shanmugam (2011), Dierssen and Smith (2000) and Siegel et al. (2013)	Hu et al. (2012)	Saitoh et al. (2002), Nezlin and Li (2003), Srokosz et al. (2004), Brickley and Thomas (2004), Navarro and Ruiz (2006), Tan et al. (2006), Henson and Thomas (2007), Marrari et al. (2008), Yoo et al. (2008), Garcia-Soto and Pingree (2009), Henson et al. (2009), Platt et al. (2009) Quartly and Srokosz (2004), Vargas et al. (2009), Song et al. (2010), Raitsos et al. (2011), Racault et al. (2012) and Kidston et al. (2013)
Surface expression (undefined)					
Coccolithophores	Iida et al. (2002), Zeichen and Robinson (2004) and Moore et al. (2012)				
Trichodesmium	Subramaniam et al. (2002) and Dupouy et al. (2011)				
Red tides/HAB		Ahn et al. (2006) and Tang et al. (2006)	Stumpf (2001)	Ahn and Shanmugam (2006) and Shanmugam et al. (2008)	Miller et al. (2006), Stumpf et al. (2003) and Tomlinson et al. (2004)

3.2. Reflectance band-ratio algorithms

In open ocean Case 1 waters, phytoplankton is the primary water constituent (Morel, 1980; Morel and Prieur, 1977); thus, Chl-a concentrations can be empirically related to the water-leaving reflectance using relationships of various forms (e.g., Matthews, 2011; Dierssen, 2010). These empirical relationships are often derived using large, sometimes global (e.g., Fargion and McClain, 2003), *in situ* datasets of coincident Chl-a and reflectance measurements. Empirical blue-green (440–550 nm) spectral band-ratios are the most common types of ocean color algorithms used for Chl-a retrievals because most of the phytoplankton absorption occurs within this portion of the visible spectrum. However, the use of visible wavelengths can be unreliable in coastal waters. In optically complex, Case 2 waters, blue-green reflectance band-ratios become less sensitive to changes in Chl-a concentrations

because increasing concentrations of color dissolved organic matter (CDOM) and total suspended matter (TSM) (e.g., Bowers et al., 1996) require the use of other spectral bands located in the red (620–700 nm) and NIR (>700 nm) (e.g., Gitelson et al., 2009) (Fig. 5).

3.2.1. Blue-green band-ratios for open and coastal ocean waters

Gordon et al. (1983, 1980) and Feldman et al. (1984) were among the first to use empirical band-ratios from CZCS spectral bands for the study of the near-surface distribution of phytoplankton blooms in the open ocean and to explore their relationships with oceanographic conditions. Many other studies used their initial work to derive global phytoplankton maps from CZCS Chl-a imagery (e.g., Banse and English, 2000, 1997, 1994; Nezlin et al., 1999; Tang et al., 1999; Fuentes-Yaco et al., 1997b). The second and third generation of ocean color sensors (Fig. 4; Fig. 5; see

Table 5

Detecting phytoplankton blooms with MODIS (cited research is indicative only).

Phytoplankton type	Reflectance classification (thresholds, anomalies)	Reflectance band-ratios	Bio-optical model or neural network	Spectral band difference	Satellite product (threshold or anomaly) and climatology, statistics
Phytoplankton bloom (undefined)		Venables et al. (2007) ^a , Acker et al. (2008) ^a , Zhao et al. (2009a) ^a , Kahru et al. (2010) ^{a,b} , Nezlin et al. (2010) ^a and Le et al. (2013)	Shang et al. (2010), Shanmugam (2011) and Mélin et al. (2011) ^a	Hu et al. (2012)	Wang and Zhao (2008) ^a , Shi and Wang (2007), Uz (2007) ^a , Peñaflor et al. (2007), White et al. (2007) ^a , Oliveira et al. (2009), Park et al. (2010a, 2010b), Raj et al. (2010) ^a , Wang et al. (2010) ^a , Li et al. (2010b) and Dasgupta et al. (2009)
Surface expression (undefined)					
Coccolithophores	Signorini and McClain (2009), Iida et al. (2012) and Moore et al. (2012)	Balch et al. (2005)			
Trichodesmium	McKinna et al. (2011)			Hu et al. (2010a)	
Red tides/HAB	Siswanto et al. (2013)	Kahru et al. (2004) and Carvalho et al. (2011)	Cannizzaro et al. (2008) ^a and Carvalho et al. (2010)	Hu et al. (2005), Ryan et al. (2009) and Zhao et al. (2010) ^b	Cannizzaro et al. (2008), Cannizzaro (2004), Hu et al. (2004), Tomlinson et al. (2008) ^a , Anderson et al. (2011), Banks et al. (2012) ^a , Shutler et al. (2012) and Kurekin et al. (2014) ^b

^a Merged with SeaWiFS.^b Merged with MERIS.**Table 6**

Detecting phytoplankton blooms with MERIS (cited research is indicative only).

Phytoplankton type	Reflectance classification (thresholds, anomalies)	Reflectance band-ratios	Bio-optical model or neural network	Spectral band difference	Satellite product (threshold or anomaly) and climatology, statistics
Phytoplankton bloom (undefined)			Uiboupin et al. (2012)	Gower et al. (2008, 2005)	Gordoa et al. (2008)
Surface expression (undefined)				Gower and King (2011a)	
Coccolithophores	Moore et al. (2012)				
Trichodesmium		Bernard et al. (2005)		Matthews et al. (2012)	
Red tides/HAB				Ryan et al. (2008) and Jessup et al. (2009)	Li et al. (2010a)

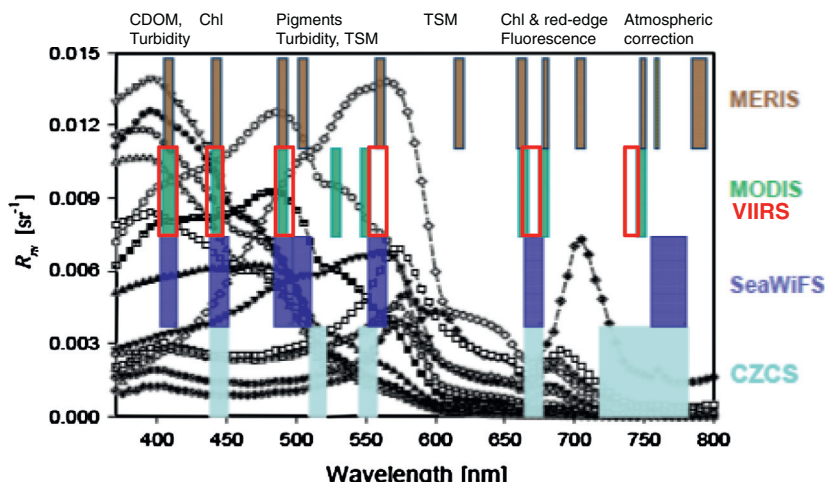


Fig. 5. Comparison of the spectral band positions for five ocean color sensors of the first (CZCS), second (SeaWiFS), third (MERIS, MODIS) and fourth (VIIRS) generations. (Figure modified from Fig. 1 of Lee et al. (2007). The authors used 14 remote sensing reflectance spectra from various waters around the world. The potential applications for each spectral region are indicated. See Table 2 as well (this review.) (For interpretation of the references to colour in this figure legend, the reader is referred to the web version of this article.)

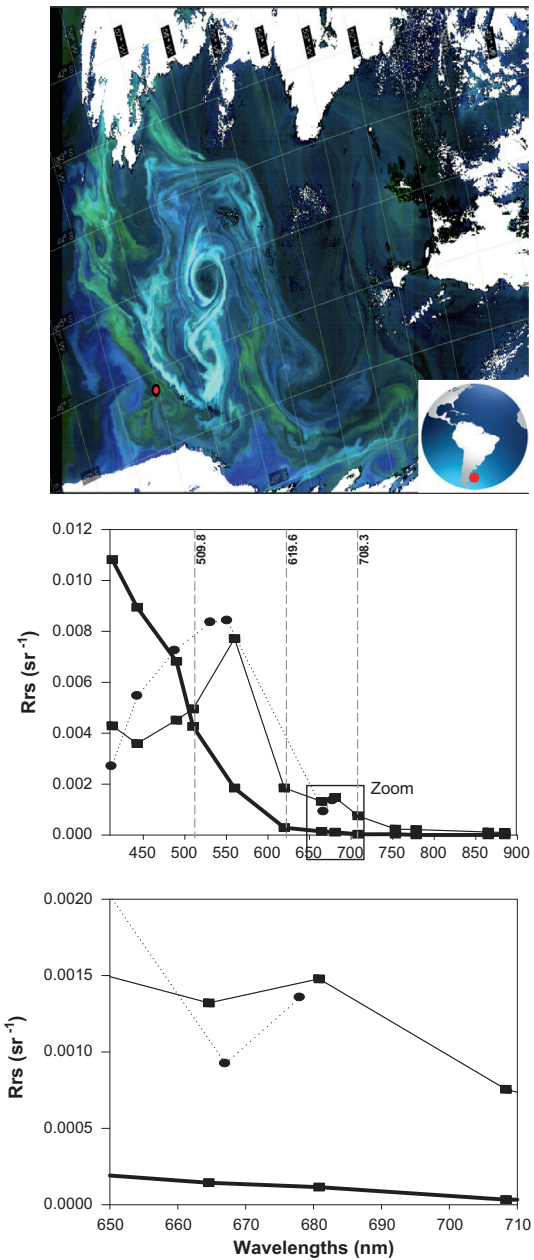


Fig. 6. Detecting algal blooms from MODIS and MERIS ocean color sensors. Top panel: RGB MERIS image of December 2, 2011 showing the pixel location (red dot) for the extracted reflectance data; middle panel: remote sensing reflectance spectra (R_{rs}) of MERIS (thin line) and MODIS (dotted line) Level 2 (standard algorithms) for the same day. Reflectance from the surrounding blue water is shown (thick line); bottom panel: zoom on the spectral region 650–710 nm. MERIS bands at 509.81, 619.30 and 708.32 nm are shown by vertical dashed lines. (For interpretation of the references to colour in this figure legend, the reader is referred to the web version of this article.)

Fig. 3 of Klemas (2012) addressed the need for more spectral bands, thereby enabling the development of more sophisticated atmospheric correction schemes and in-water constituent retrieval algorithms, which are required for both improved retrieval accuracy for water quality variables and algal bloom proxies in coastal ocean waters. SeaWiFS OC4 (O'Reilly et al., 2000, 1998) and MODIS OC3M (Campbell and Feng, 2005b, 2005a) are switching band-ratio algorithms that use spectral bands in the blue and green regions of the visible spectrum to estimate Chl-a concentrations. The MODIS OC3M (e.g., Chen and Quan, 2013) is extended from the SeaWiFS

OC4 and adapted to the MODIS spectral bands. The use of global standard ocean color band-ratios has been demonstrated to significantly overestimate Chl-a. Moore et al. (2009) have shown that the nominal uncertainty of 35% for Chl-a retrievals is true in ocean gyres, but the OC3M relative Chl-a error is >50% outside those gyres and can be >100% in coastal waters. Komick et al. (2009) found that MODIS OC3M systematically overestimated Chl-a when lower than 0.13 mg m^{-3} in Western Canadian waters. Similar results were also found by Radenac et al. (2013) for the equatorial Pacific warm pool. For SeaWiFS OC4, Volpe et al. (2007) found that Chl-a was overestimated by 70% for Chl-a levels lower than 0.2 mg m^{-3} in the Mediterranean Sea. Such low Chl-a concentrations are encountered in the vast majority of the global ocean (Hu et al., 2012).

3.2.2. The relevance of the red-NIR spectral regions in coastal waters

The *in vivo* absorption peak near 676 nm is minimally affected by the influence of CDOM and TSM when the two are in low concentrations (see Section 3.3; Fig. 5). Spectral bands near 676 nm have been widely used for the retrieval of Chl-a in coastal waters (Odermatt et al., 2012; Gurlin et al., 2011). Gitelson et al. (1999) have shown that reflectance increases in the NIR beyond 700 nm due to increased scattering from algal biomass, correlated to an increase in Chl-a for most phytoplankton groups. The sensitivity analysis conducted by Ruddick et al. (2001) on two red-NIR band-ratio algorithms revealed that the relative error on Chl-a retrievals became more significant at low Chl-a concentrations ($<10 \text{ mg m}^{-3}$) and in low backscatter conditions but also that the choice of paired wavelengths was very important. Their study showed that a band-ratio algorithm that uses the red-NIR band pair 672 and 704 nm would perform best at Chl-a $\sim 10 \text{ mg m}^{-3}$, whereas a wider red-NIR band pair spreading further apart (e.g., 667 and 748 nm) would perform best at Chl-a $\sim 100 \text{ mg m}^{-3}$.

The “red-edge” is technically defined as an increase in spectral reflectance in the red-NIR (680–750 nm) and often results from the presence of partly submersed vegetation (e.g., Dierssen et al., 2007, 2006; Bostater et al., 2003; Gitelson, 1992) or algal bloom surface expressions (e.g., Shen et al., 2012; Ruddick et al., 2008) (Fig. 5). Only a few ocean color sensors have the spectral requirements that enable the detection of those reflectance features. For SeaWiFS, two of the nine spectral bands are positioned in red-NIR region of the spectrum (namely 670 nm and 765 nm), and these two bands have limited use for the detection of Chl-a. In contrast, MODIS and MERIS provide more spectral bands between 600 and 800 nm (Figs. 5 and 6). Further useful applications of the red-NIR spectral region in reflectance-based algorithms are discussed in Sections 3.3 and 4.

3.2.3. Band-ratio algorithms: Limitations and challenges

Most reflectance band-ratios are designed for global applications over optically deep ocean waters (Odermatt et al., 2012). The use of band-ratios often leads to erroneous retrievals in coastal waters, where the optical complexity is highly variable (Dierssen, 2010; Blondeau-Patissier et al., 2004). Additional limitations in the use of band-ratios are regional differences in optical properties and concentrations; the generalized global parameterization of some algorithms is inapplicable in some of the world's ocean regions (e.g., Volpe et al., 2007; Clastre and Maritorena, 2003; Sathyendranath et al., 2001; Dierssen and Smith, 2000). Many studies have shown that the retrieval accuracy of Chl-a by satellite ocean color sensors, aimed to be within $\pm 35\%$ in oceanic waters, cannot always be met when using band-ratio algorithms (e.g., Moore et al., 2009; Hu et al., 2000). In coastal waters, the quality of this retrieval significantly degrades and is often considered unreliable. The use of blue-green spectral bands for the specific detection of Chl-a in coastal waters is affected by the absorption signal of CDOM and TSM (e.g., Dierssen, 2010; Gower, 2000;

Joint and Groom, 2000). To overcome this limitation, other studies suggested the use of red-NIR band-ratios for Chl-a retrieval in coastal waters (e.g., Moses et al., 2012; Shanmugam, 2011).

3.3. Spectral band difference algorithms

Spectral band difference algorithms exploit spectral regions that feature significant changes in the reflectance spectrum due to the presence of an algal bloom, compared to the nearby bloom-free water. Given that absorption tends to vary more rapidly with wavelength than scattering, two adjacent reflectance spectral bands may have similar backscattering properties but will differ significantly in absorption. Hence, this absorption feature can be quantified by spectral difference. The various forms of spectral band difference algorithms use band triplets from the red-NIR or the blue-green spectral regions (Table 2) depending on whether the algorithm is designed to be sensitive to an algal group, high chlorophyll concentrations or surface bloom expressions (Fig. 7). One of the most used ocean color spectral band difference algorithms is the Fluorescence Line Height (FLH) (see review of Xing et al. (2007)), an index for quantifying solar-induced chlorophyll

fluorescence. Other similar mathematical expressions are used to derive algal bloom indices from SeaWiFS, MERIS and MODIS (Table 2) and are discussed in this section.

3.3.1. Fluorescence Line Height (FLH)

The literature published on this topic since the 1960s (Yentsch and Menzel, 1963) has shown that estimating fluorescence is greatly beneficial to studies of phytoplankton biomass (Falkowski and Kiefer, 1985), physiology (e.g., Westberry et al., 2013; Behrenfeld et al., 2009), and composition (e.g., Hu et al., 2005). The remote sensing approach used to retrieve FLH was originally developed by Neville and Gower (1977), and its first application to an ocean color sensor was on MODIS-Terra (Abbott and Letelier, 1999; Letelier and Abbott, 1996). It is well known, however, that MODIS-Terra suffers from uncertainties and instabilities, particularly the radiometric response of the 412-nm band, which has significantly (>40%) degraded since the start of the mission (Franz et al., 2008). The significant striping in MODIS-Terra water-leaving radiances makes the data largely unusable. Thus, MODIS mostly refers to the sensor on the Aqua satellite. The spectral band positions of MERIS (Gower et al., 1999) and MODIS (Hoge et al., 2003) allow

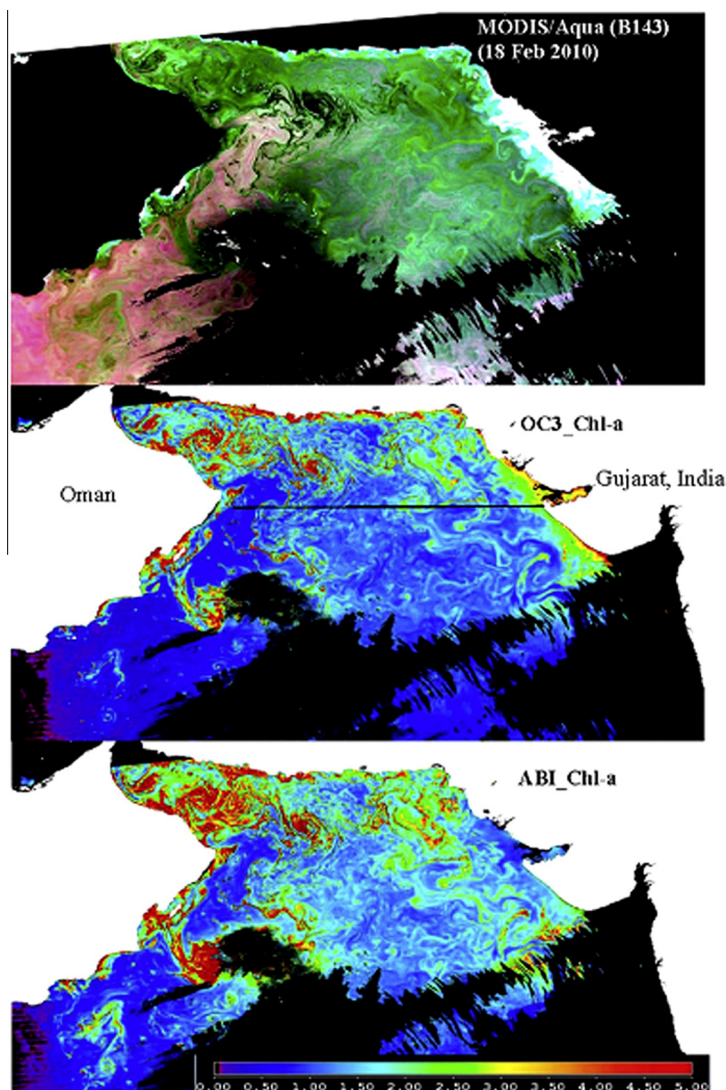


Fig. 7. The Algal Bloom Index (ABI) is used to map phytoplankton blooms in the Arabian Sea and the Gulf of Oman from a MODIS-Aqua scene of February 28, 2010. Fig. 4 from Shanmugam (2011). Top panel: A MODIS/Aqua true color composite on 18 February 2010 in the Arabian Sea and Gulf of Oman; The corresponding Chl-a images are derived using (middle) the OC3 and (bottom) ABI algorithms.

for the computation of FLH, but this product cannot be derived from CZCS, SeaWiFS and VIIRS because of the lack spectral bands in the 670–690 nm range. Gower and Borstad (2004) and Zhao et al. (2010) compared FLH results between MODIS and MERIS and concluded that MERIS bands were better positioned for measuring fluorescence. The use of MODIS FLH to detect HAB has been successfully used by many (Frolov et al., 2013; Cannizzaro et al., 2008; Hu et al., 2005), providing more reliable information than a standard Chl algorithm. MERIS FLH was found to be successful at detecting high biomass phytoplankton in sediment-dominated coastal waters (e.g., Gower et al., 2005). However, others studies have led to inconclusive results on the benefits of FLH in the detection of algal blooms (e.g., Tomlinson et al., 2008).

3.3.2. Maximum Chlorophyll Index (MCI)

The Maximum Chlorophyll Index (MCI) can only be applied to MERIS because of its use of the 708.75 nm band. This band is more responsive to strong reflectance in the NIR, and the lack of similar bands in MODIS and VIIRS may hamper the detection of high-concentration bloom events. The MCI is mainly designed for the detection of high-concentration algal blooms, and it was successfully used to globally monitor phytoplankton blooms in the world's oceans by Gower et al. (2008). The minimum Chl-a concentration required for a phytoplankton bloom to be detected by the MCI is $\sim 30 \text{ mg m}^{-3}$ (Gower et al., 2005), but phytoplankton blooms can have much higher concentrations, with some studies reporting $\text{Chl-a} > 200 \text{ mg m}^{-3}$ (e.g., Gower and King, 2007a; Sasamal et al., 2005).

3.3.3. Floating Algae Index (FAI) and Scaled Algae Index (SAI)

Hu et al. (2010c) and Hu (2009) proposed the Floating Algae Index (FAI) to detect large ($>4000 \text{ km}^2$) surface-floating algae from MODIS 250 and 500 m bands in both fresh and marine environments. The FAI uses a functional form similar to FLH and MCI where the height of the NIR peak is estimated relatively to a linear baseline from adjacent bands in the red and short wave infrared (SWIR) wavelengths (Table 2). Thus, the FAI is sensitive to the red-edge and is robust to the influence of CDOM, aerosols and sun glint because of the use of NIR bands. However, similarly to MCI, the FAI is likely sensitive to turbid waters and shallow depths. It is used in combination with pre-determined thresholds to help separate land, cloud and high concentrations of submersed algae or sediments from pixels associated with surface algae scums. FAI was originally applied to the detection of cyanobacteria and macro-algae in the freshwater lake Taihu and the Yellow Sea (China). Its global applicability remains untested. Building on this research, Garcia et al. (2013) developed an automatized image processing algorithm, the Scaled Algae Index (SAI), which is a necessary intermediate product for quantifying the spatial coverage of the floating macro-algae observed in satellite imagery based on FAI.

3.3.4. Color Index Algorithm (CIA)

A recent development in algal bloom indices is the Color Index Algorithm (CIA) proposed by Hu et al. (2012). This empirical algorithm was originally developed to estimate surface Chl-a concentrations in oligotrophic ($\leq 0.25 \text{ mg m}^{-3}$) waters. The CIA is a three-band reflectance difference algorithm (443 nm, 555 nm and 670 nm bands), making it applicable to SeaWiFS, MODIS and MERIS. Its accuracy has not yet been fully validated because of the lack of low-concentration, high-quality *in situ* Chl-a data from the world's oceans. The CIA was successfully applied to the waters of the Red Sea by Brewin et al. (2013), where it was found to perform better than the MODIS OC3 at retrieving Chl-a because of the low concentrations typically encountered in those waters.

3.3.5. Spectral band difference algorithms: Limitations and challenges

Many limitations in the use of red-NIR bands have been raised in this section. The robust application of FLH for the detection of algal blooms remains under discussion. McKee et al. (2007) suggested that the FLH signal could be masked in complex coastal waters due to the influence of CDOM and TSM. Similarly, Gilerson et al. (2007, 2008) found that MODIS FLH retrieved fluorescence with reasonable accuracy only for waters with $\text{Chl} < 4 \text{ mg m}^{-3}$ but that the signal was masked by particulate backscattering in turbid waters with high CDOM and TSM concentrations. The authors also questioned the performance of the MERIS FLH algorithm in coastal waters where large errors could be introduced via the linear baseline between the two NIR MERIS bands. The use of a linear baseline between the two NIR MERIS bands for the computation of FLH has been demonstrated to work in coastal waters with Chl-a concentrations of up to 20 mg m^{-3} (Gower and King, 2007b) (Fig. 8). For higher chlorophyll concentrations however, due to the combined effects of water absorption and Chl-a distortion, the Chl-a spectrum and a linear baseline can no longer be used. Gower et al. (1999) also challenged the theory that the scattering by TSM had a significant reducing effect on the relative fluorescence height above the baseline. The influence of CDOM on the FLH is often considered small in relatively low concentrations due to its negligible absorption in the NIR. Hu (2009) acknowledged that limitations in the MODIS FAI included the questionable reliability of the MODIS atmospheric correction and the lack of a MODIS-cloud masking algorithm that would reliably flag all cloud and/or sun-glint contaminated pixels while keeping (floating) algae pixels. Although the first issue can be easily solved using Rayleigh-corrected reflectance (Hu et al., 2010b), the second remains a problem, and the author suggested the use of true-color FAI-paired images to separate the clouds from the ocean surface features. Several ocean color algal bloom indices can be combined to enhance our interpretation of algal bloom phenomena and their underlying mechanisms (see Section 5.3).

3.4. Bio-optical models

Bio-optical models are based on various fundamental theories of marine optics and, because they rest on firm theoretical bases and rigorous equations, they are often robust (e.g., Morel, 2001). Coastal systems are generally shallow ($<100 \text{ m}$), dynamic, transitional environments that receive considerable amounts of freshwater inputs carrying nutrients, dissolved and particulate organic matter, sediment and contaminants (Blondeau-Patissier et al., 2009; Babin et al., 2003). Extracting detailed and accurate information from ocean color imagery is a more challenging task in coastal

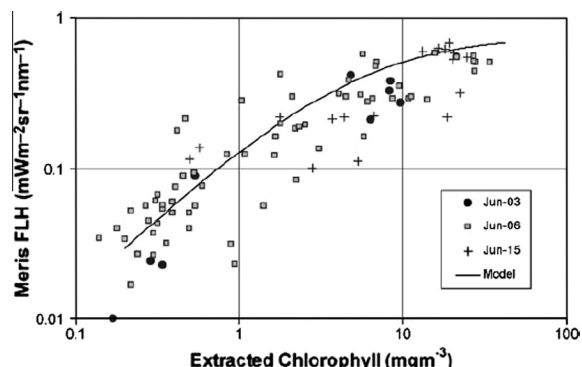


Fig. 8. The MERIS FLH product as a function of surface extracted chlorophylls from the Canadian west coast, ECOHAB project, June–September 2003. Fig. 4 of Gower and King (2007b).

waters in comparison to the open ocean (Tilstone et al., 2011b; Qin et al., 2007). Inversed modeling algorithms (Odermatt et al., 2012) are often necessary to enable the accurate retrieval of Chl-a concentrations in optically complex waters, although optically active constituents (CDOM, TSM) may show discernible patterns of their own during algal bloom conditions (e.g., Chari et al., 2013; Zhao et al., 2009b).

3.4.1. Retrieval of taxa-specific pigment concentrations from bio-optical models

Taxonomic phytoplankton groups contain different combinations of pigments (e.g., Uitz et al., 2006), but the spectral features of individual pigments are often similar (e.g., Aiken et al., 2008; Richardson, 1996). There is still some debate about which phytoplankton pigments can be reliably identified because many water quality parameters confine the algorithms to specific conditions. However, the use of the (specific) absorption coefficient of phytoplankton indexed to the composition of the phytoplankton community sampled *in situ* has brought promising results in open ocean waters (e.g., Claustre et al., 2005; Sathyendranath et al., 2004). Such techniques are employed to detect phytoplankton community structures from ocean color datasets (e.g., Brewin et al., 2011), but significant progress is yet to be made, both in the bio-optical models and databases, for their use in coastal waters.

3.4.2. Derivation of inherent optical properties from bio-optical models for the detection of algal blooms

The principal phytoplankton pigments that mostly contribute to absorption are the photosynthetic pigments consisting of the chlorophylls, carotenoids and biliproteins. The phytoplankton absorption coefficient is an important parameter in ocean color algorithms and is increasingly used to parameterize algal bloom algorithms (e.g., Goela et al., 2013). To study the phytoplankton dynamics characterizing the coastal waters of the Taiwan Strait, Shang et al. (2010) used the Quasi-Analytical Algorithm (QAA) from Lee et al. (2002) to retrieve the phytoplankton absorption coefficient from MODIS. Their findings promoted the use of the phytoplankton absorption coefficient over Chl-a because the latter can suffer from the contamination of non-biotic optically active material.

3.4.3. Bio-optical models: Limitations and challenges

Bio-optical forward and inverse modeling is developing rapidly as an essential tool to understand the effects of dense algal concentrations on light absorption and backscattering coefficients. False positive bloom detections in CDOM- or TSM-rich waters and uncertainties due to the quality of the atmospheric correction are still hampering accurate retrievals of optical properties and biogeochemical concentrations in coastal waters. The use of specific inherent properties now has a central role in bio-optical modeling (e.g., Brando et al., 2012; Tilstone et al., 2011a), but the identification of specific phytoplankton groups on the basis of inherent optical properties remains a challenge in coastal waters. For future parameterizations of taxa-specific bio-optical models, Claustre et al. (2005) stressed the need to make coincident measurements of the phytoplankton taxonomic composition, photophysiological parameters and phytoplankton absorption to improve local, regional and global *in situ* databases. As suggested by Dierssen (2010) and later by Sen Gupta and McNeil (2012), the water properties of the world's oceans are changing. It is probable that algorithm parameterizations derived from *in situ* data collected over the past decades might not be applicable in the near future due to the possible change in the CDOM-Chl relationships in coastal waters. One of the latest reports on future ocean color mission requirements, IOCCG Report 13 (2012b), stated that "phytoplankton blooms"

timing, frequency, composition and intensity are expected to change with climate in ways that may be hard to predict. (...) Thus reliable and accurate detection of algal blooms is an objective for future missions" (p. 14).

4. The detection of specific types of algal blooms

4.1. Algal blooms with surface expressions

Algal blooms with surface expressions, such as coccolithophores, cyanobacteria and *Sargassum*, are observable in satellite imagery due to the large areas they often cover (Fig. 1). Spectral characteristics specific to those taxa may be exploited for their mapping, or masking, by using empirically derived, rule-based reflectance classification algorithms; bio-optical models can also be used.

4.1.1. Coccolithophore blooms

Coccolithophores, with the globally dominant *Emiliania huxleyi*, are calcifying phytoplankton species that form large, dense blooms occurring at most latitudes (Brown, 1995). Coccolithophore blooms play an important role in ocean biogeochemistry (Harlay et al., 2011) and the upper ocean light field (e.g., Balch et al., 2005). The senescent stage of Coccolithophore blooms is often identifiable in an ocean color remote sensing image by its milky blue-green color (Fig. 1), accompanied by the typical high scattering across all spectral bands (400–800 nm) that results from the detached coccoliths (Voss et al., 1998). Following the early work of Holligan et al. (1983), who reported on the higher reflectance values found for CZCS satellite image pixels within Coccolithophore-rich waters, Brown and Yoder (1994a) and Brown (1995) pioneered research on the detection of Coccolithophore blooms. Using a reflectance classification technique to map those events in the global ocean, Brown and Yoder (1994a), Ackleson et al. (1994) and, later, Merico et al. (2003) identified many limitations that were associated with this technique, including false positives resulting from various sources, such as poor satellite coverage, atmospheric correction errors, reflectance signal contamination from CDOM and scattering from resuspension of TSM. These contaminating sources, whether individual or combined, could bias the results obtained not only for the detection of Coccolithophore blooms but also those of Chl-a (e.g., Blondeau-Patissier et al., 2004). Nonetheless, the acceptable accuracy of the classification results led to the documentation of Coccolithophore bloom events at both global (e.g., Brown, 1995) and basin scales (e.g., Brown and Podesta, 1997; Brown and Yoder, 1994b). Since this early work with CZCS (Table 3), novel methods have been developed using reflectance anomalies (e.g., Shutler et al., 2010) and reflectance classifiers (e.g., Moore et al., 2012) with SeaWiFS (Table 4), MODIS (Table 5) and MERIS (Table 6). These new approaches allowed for the mapping of Coccolithophore blooms in ocean regions where previously such blooms were either not detected or underestimated, such as shelf or polar seas (e.g., Holligan et al., 2010; Hegseth and Sundfjord, 2008). The use of existing standard Coccolithophore masks in those regions is often unsuitable, and some regional adjustments are required. Iida et al. (2002) demonstrated that the thresholds used in the NASA standard SeaWiFS Coccolithophore mask algorithm were too high to map the events in the Bering Sea and lower threshold values were necessary.

4.1.2. *Trichodesmium* blooms

Blooms of cyanobacterium *Trichodesmium* fix atmospheric nitrogen into ammonium, making it usable for other organisms (e.g., LaRoche and Breitbarth, 2005). Subramaniam and Carpenter (1994) qualitatively mapped *Trichodesmium* sp. blooms from CZCS satellite imagery of the Atlantic, Indian and Pacific Oceans using an

empirical reflectance algorithm based on their high reflectivity. Due to the strong absorption by phycoerythrin, *Trichodesmium* blooms have a characteristic spectral feature at 550 nm that makes them potentially identifiable in satellite reflectance spectra. Bio-optical properties specific to *Trichodesmium* were also used by Subramaniam et al. (1999a,b) for the large-scale detection of such events in AVHRR imagery off the Somali coast from a reflectance-based model. Those properties were subsequently used in a semi-empirical bio-optical model by Subramaniam et al. (2002) to detect *Trichodesmium* events in SeaWiFS imagery off the South Atlantic Bight, demonstrating that *Trichodesmium* blooms could be detected in optically complex coastal waters when in sufficient quantity. However, this model had some limitations, including sensitivity to bottom reflection and corals and generating false positives from other similarly reflective sources (such as Coccolithophore or *Phaeocystis* blooms, TSM). Recent studies employ criterion-based reflectance techniques to detect and quantify *Trichodesmium* floating mats using reflectance anomalies (Dupouy et al., 2011, 2008), high-resolution NIR bands (McKinna et al., 2011) and blue-green reflectance bands with MODIS. Hu et al. (2010a) demonstrated the potential of MODIS FAI to distinguish *Trichodesmium* mats from the background influence of both TSM and CDOM in the coastal waters of Florida, on the condition that *Trichodesmium* was in sufficiently high concentration (i.e., Chl-a > 4 mg m⁻³). Mostly a qualitative approach (e.g., presence/absence), very few of these reflectance-based studies provide quantitative estimates of *Trichodesmium* blooms from satellite imagery. The quantitative estimate of *Trichodesmium* sp. abundances can be achieved with the use of taxa-specific pigment retrieval models. Westberry et al. (2005) used an extension of the bio-optical model of Garver and Siegel (1997) and Maritorena et al. (2002) (GSM) to map the abundance and biomass of *Trichodesmium* on a global scale from SeaWiFS imagery. These two studies helped reveal many aspects of the distribution of *Trichodesmium* sp. in the global ocean, with the largest annual spatio-temporal occurrence of *Trichodesmium* sp. in the Pacific Ocean.

4.1.3. Floating Sargassum

Sargassum sp. are surface-floating macro-algae distributed throughout the temperate and tropical oceans. *Sargassum* sometimes cover large areas (tens of kilometers), which may provide a useful proxy for tracking convergent or divergent oceanographic processes (e.g., Zhong et al., 2012). MERIS MCI and MODIS FLH have been shown to be very effective in monitoring their distributions in the Gulf of Mexico and the North Atlantic Ocean (Gower and King, 2011b, 2008; Gower et al., 2006). Using those surface expression indices, Gower and King (2011b) have shown that *Sargassum* sp. seasonal occurrences are characterized by a migration from the Gulf of Mexico in spring to the North Atlantic in July, ending near the Bahamas in February of the following year. An estimated biomass of floating *Sargassum* of 1 g Chl kg⁻¹ wet algae (Gower et al., 2006) corresponds to 10⁶ ton yr⁻¹ sourced from the Gulf of Mexico, which may have large implications for carbon fluxes (Gower and King, 2011b). The spatial and seasonal distributions of *Sargassum* have, overall, been well mapped using satellite imagery, but Gower et al. (2013) recently showed a large drift in their distributions for the year 2011, the cause of which is unclear.

4.1.4. Harmful Algal blooms – Example of dinoflagellate *Karenia brevis*

The outbreak of a single, dominating phytoplankton species can alter coastal ecosystems, often causing costly damages to both the local economy and the marine ecosystem (e.g., Babin et al., 2008; Hu et al., 2004). Harmful algal blooms are often referred to as red tide events, but a reddish appearance of the ocean water can be caused by any phytoplankton species, with the only variable being its concentration (Kutser, 2009; Dierssen et al., 2006).

Red-tide-type phytoplankton species, such as dinoflagellate *Karenia brevis*, absorb radiations in the blue and lower green regions (450–500 nm) of the visible spectrum while strongly reflecting radiations in the yellow region (570–580 nm). Bernard et al. (2005) used an empirical Chl-a algorithm based on the ratio between the MERIS red bands 665 and 709 nm to detect high biomass (up to 200 mg m⁻³) dinoflagellate-dominated HAB events in the Southern Benguela. Another band-ratio was proposed by Ahn and Shanmugam (2006). The Red Tide Index (RI) is specifically designed to detect red-tide blooms (Table 2). The Red Tide Index Chlorophyll Algorithm (RCA) empirically relates RI to Chl-a for concentrations of up to 70 mg m⁻³ (see Fig. 6 from Ahn and Shanmugam (2006)). Their findings showed that spatial patterns of red-tide blooms as mapped from the RI and RCA indices were more consistent with field observations than when standard band-ratio algorithms were used. In this case, Ahn and Shanmugam's (2006) study demonstrated the successful application of the band-ratio approach over bio-optical models such as the one developed by Cannizzaro et al. (2008) for the Gulf of Mexico from SeaWiFS and MODIS imagery. Band difference algorithms are also used. The Red Band Difference (RBD) proposed by Amin et al. (2009a, 2009b) is an index specifically designed to detect *K. brevis*. The spectral region used for the RBD (665–681 nm) is sensitive to both phytoplankton absorption and scattering from suspended sediment; thus, an additional discrimination algorithm is required, the *Karenia brevis* Bloom index (KBBI) (Amin et al., 2008; Table 2). KBBI is the ratio of the RBD to the sum of the same two normalized water reflectance bands. This procedure can be applied to both MODIS and MERIS and has been demonstrated to work in waters other than the Gulf of Mexico (e.g., Gulf Stream, mid-Atlantic).

5. Statistical techniques and data assimilation to assess phytoplankton bloom dynamics

The mapping of the seasonal, inter-annual, or decadal cycle of phytoplankton growth, which can include its spatial patterns, timing and magnitude, is key to understanding algal bloom dynamics in a specific ocean region. The sole use of an ocean color dataset is often insufficient for accurately resolving ocean color constituents (e.g., Mélin et al., 2011; Zingone et al., 2010; Uz, 2007), and additional data sources from models (e.g., Mouw et al., 2012) or non-ocean color satellite sensors (e.g., Robinson et al., 2004; Saitoh et al., 2002) can be necessary. In addition, statistical techniques are often used as a post-processing step to unravel the temporal and/or spatial patterns of those events (e.g., Kurekin et al., 2014). The comprehensive reviews of Bierman et al. (2011) and Kitsiou and Karydis (2011) already described the univariate and multivariate statistical techniques that can be applied to water quality data. Klemas (2012) and Brody et al. (2013) used case studies to illustrate the applications of remote sensing techniques for the detection of phytoplankton blooms. This section provides additional material to these reviews and explores the various statistical techniques that can be employed to extract further information from satellite-derived climatologies and time-series.

5.1. Statistical partitioning of marine ecosystems

To analyze the dynamics of phytoplankton blooms in a study region, it is often necessary to first partition it into sub-regions (IOCCG Report 9, 2009). The fundamental difference between the partition of terrestrial and aquatic ecosystems is that aquatic ecosystems usually have dynamic boundaries between biomes to account for seasonal or inter-annual variations (Platt and Sathyendranath, 1999). Longhurst (1995) was among the first to provide a classification of the oceanic pelagic environment based

on the spatial variability of the ocean's physical properties. Other work has followed using satellite-derived Chl-a as the main variable to characterize the spatial distribution, areal extent and dynamics of phytoplankton blooms using multivariate statistical analysis (e.g., Brickley and Thomas, 2004; Fuentes-Yaco et al., 1997a). Hardman-Mountford et al. (2008) used six years of SeaWiFS Chl monthly global composites and Principal Component Analysis (PCA) to characterize broad-scale ecological patterns in the world's oceans. Their classification, based on the Chl spatial distribution and variability, was consistent with Longhurst's grouping of four primary biomes, although a major difference emerged for the equatorial biome. The delineation of ecosystem boundaries can be performed using clustering methods (e.g., K-means and Empirical Orthogonal Functions) to describe the spatial and temporal variability of a study region (e.g., Bergamino et al., 2010; Henson and Thomas, 2007; Brickley and Thomas, 2004) (Fig. 9).

5.2. Time-series, fitted models and signal processing techniques

The statistical analysis of algal biomass cycles using time-series can help detect trends in a dataset or reveal correlations between the dynamics of phytoplankton biomass and environmental factors that may be inherent to a study region.

A special issue of the journal *Estuaries and Coasts* (Zingone et al., 2010) was dedicated to the analysis of multi-scale phytoplankton variability for 22 coastal ecosystems around the world by means of 84 timeseries, some of which were computed from remote sensing data. This special issue highlighted the power of time-series analysis as a statistical technique for deriving environmental baselines. Although SeaWiFS, MODIS-Aqua and MERIS individually have at least a decade of ocean color data, multiple-sensor data merging is often required to significantly

extend the timeseries. Maritorena et al. (2010) showed that over a seven year-period, the average daily coverage of the world's ocean was ~25% when a merged satellite product was used, almost double the global coverage of any single mission. Kahru et al. (2010) merged data from SeaWiFS, MERIS and MODIS-Aqua to examine the timing of the annual phytoplankton bloom maximum in the Arctic. The data merging of satellite-derived surface Chl-a extended their time series as far back as 1997 (Tables 1 and 5). The authors found significant trends towards earlier phytoplankton blooms in ~11% of their study area.

The analysis of timeseries can be approached using time-domain methods or mixed time-and frequency-domain methods. The first technique analyzes data series in the same space in which they were observed, whereas the second decomposes data series at different time scales and frequencies. The sole use of frequency-domain approaches for time-series analyses of phytoplankton biomass is not common. In the timedomain, the timeseries is decomposed into individual, periodic oscillations, the sum of which matches the original signal. Platt et al. (2009) and Song et al. (2010) qualitatively analyzed the timeseries of SeaWiFS data of Chl-a for 10 regions of the Northwest Atlantic Ocean over a 10-year period (1998–2007) with a time-domain approach. To quantify the timing of the spring and summer blooms, they fitted a shifted-Gaussian model to the satellite-derived chlorophyll data using a non-linear least-squares method. They found that blooms in some regions occurred consistently earlier than their expected latitudinal norm.

Mixed time-frequency statistical techniques include the Empirical Mode Decomposition (EMD) (Huang et al., 1998), a signal processing technique that is datadriven and decomposes an initial signal into several high- and low-frequency oscillation components, or wavelets (e.g., Demarcq et al., 2012; Nezlin and Li,

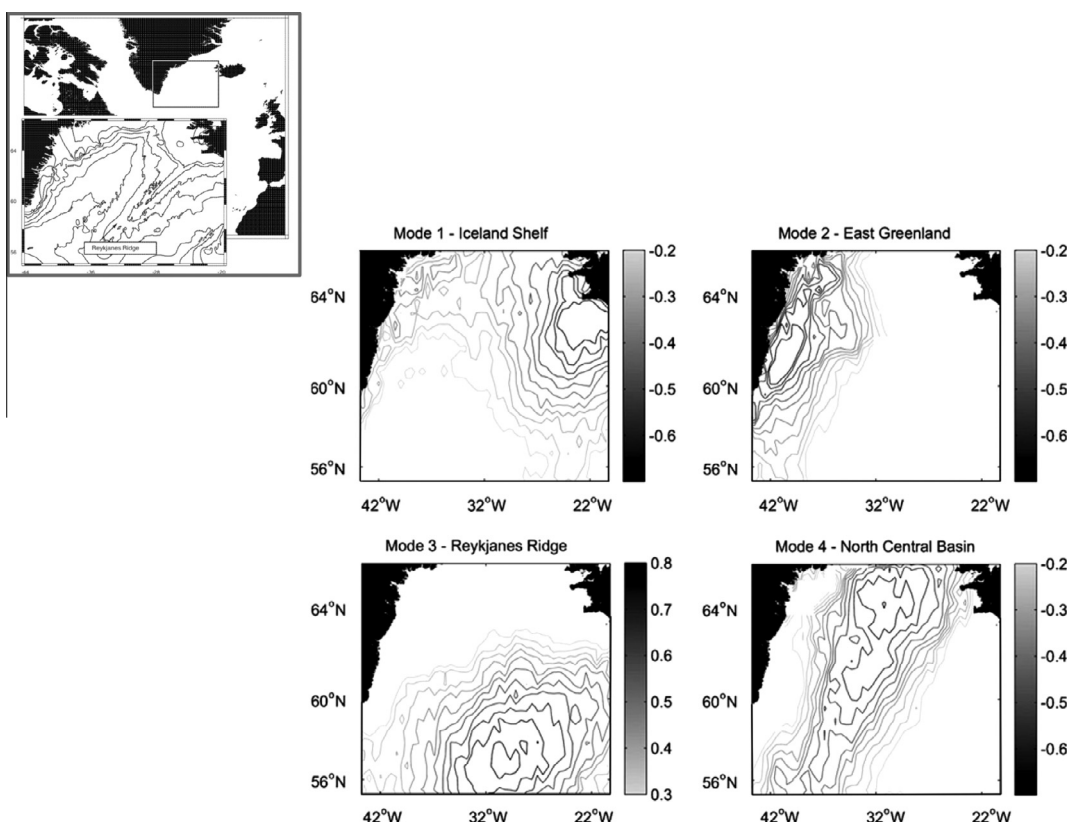


Fig. 9. Use of multivariate statistical analysis and satellite ocean color data to define biogeographic zones. The biogeographic zones of the Irminger Basin (top panel) are determined by an EOF analysis of the SeaWiFS chlorophyll-a concentration. The four modes are presented as homogenous correlation maps. Only contours for which the correlation is statistically significant ($p < 0.01$) are plotted. Figs. 1 and 2 from Henson et al. (2006).

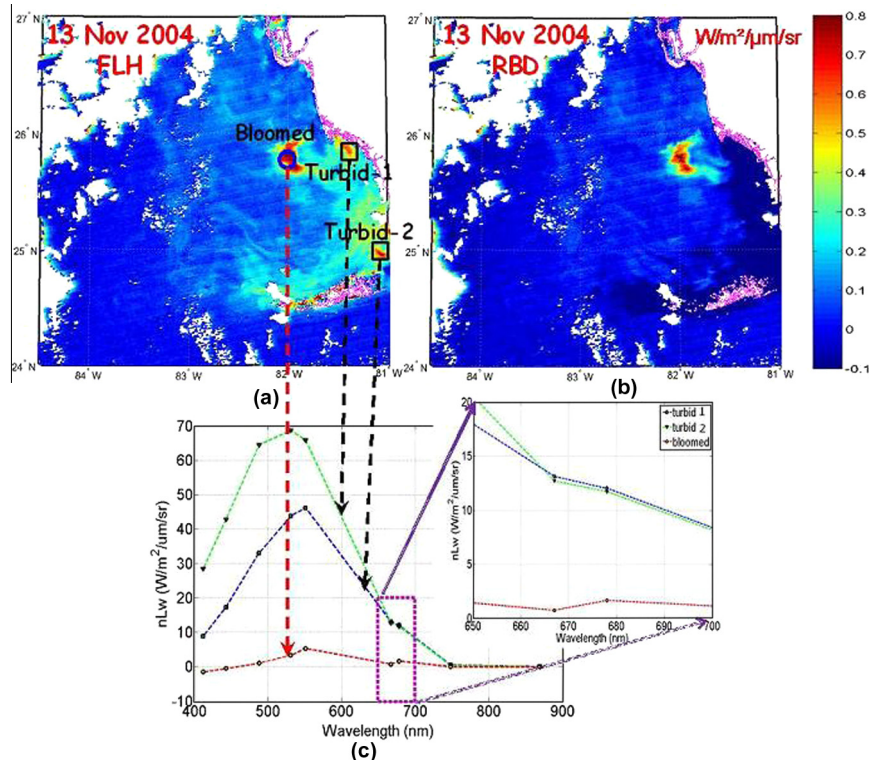


Fig. 10. Detecting *Karenia brevis* blooms in a MODIS-Aqua image of November 13, 2004 in west Florida shelf waters using FLH and RBD (both in $\text{W m}^{-2} \mu\text{m}^{-1} \text{sr}^{-1}$) (Amin et al. (2009b), Fig. 6).

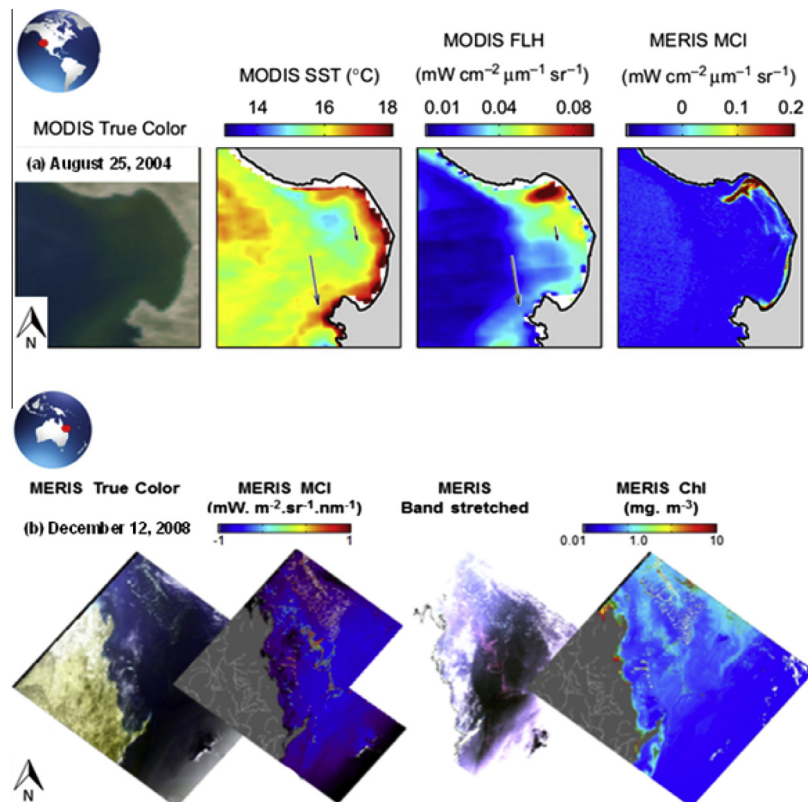


Fig. 11. Combining multiple satellite products to identify algal blooms: Top panel: Detecting a red-tide bloom in Monterey Bay, California on August 25, 2004 from MODIS and MERIS products (Fig. 4 from Ryan et al. (2009)); Bottom panel: detecting a surface algal bloom (~500 km long), possibly of *Trichodesmium sp.*, off the Fitzroy River on December 12, 2008 (Great Barrier Reef, South east coast of Australia; 22–26°S) from two MERIS satellite products and a band-stretched image (Blondeau-Patissier (2011)). (For interpretation of the references to colour in this figure legend, the reader is referred to the web version of this article.)

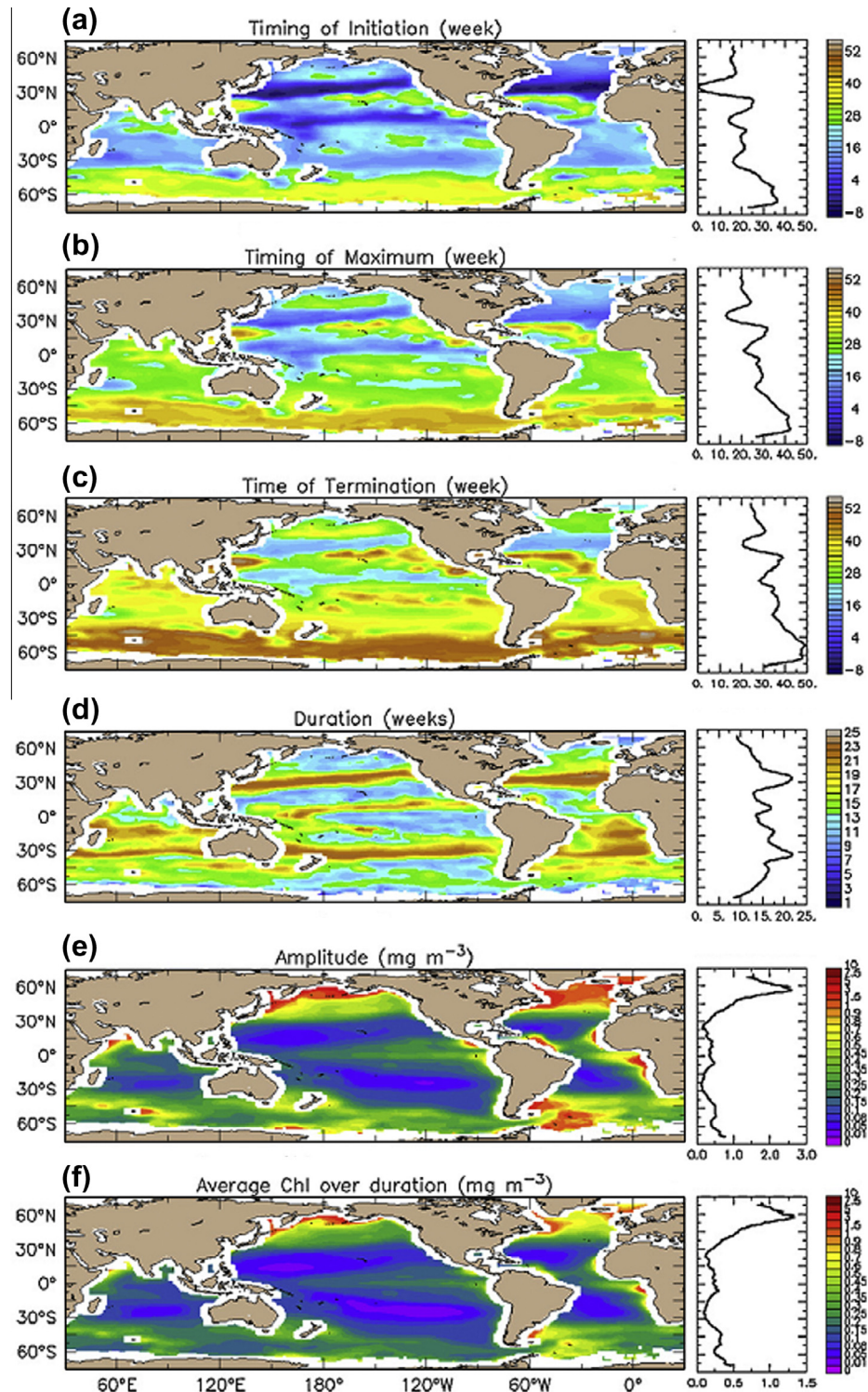


Fig. 12. Seasonal timing of phytoplankton on a global scale. The spatial distributions are averaged over 10 years of SeaWiFS data (1998–2007). The right panels show the data averaged longitudinally and smoothed latitudinally with a 5° running average. The negative sign in panels (a–c) is due to the growing period spanning the calendar year. Fig. 1 from Racault et al. (2012).

2003). These components are used to reveal temporal features in noisy timeseries. Wavelet- and variance-preserving spectra, as well as Lomb-Scargle periodograms (Scargle, 1982), are similar to the Fourier Transform. They are used for the detection of cyclic periods of unevenly spaced datasets (e.g., Yoo et al., 2008), which typically include those from ocean color satellites because data gaps can

originate from the lack of ocean color sensors (Fig. 4) or from the presence of clouds.

As ocean color satellite data time-series become longer (>10 years of continuous data), time-series analysis techniques will make it possible to more reliably assess the periodicity characterizing the datasets of a specific region. As such, trends in

satellite-derived information on phytoplankton are used as a link to possible climate and ecosystem changes.

5.3. Satellite product climatologies and merging data from multiple sources

Satellite data climatologies are commonly derived from a three-dimensional datacube (latitude, longitude, time) of a satellite product, allowing the analysis of the selected product through both time and space. Each layer of the datacube is mapped over the same longitude–latitude grid and can be composed of daily satellite images, or composites of various lengths. The use of chlorophyll climatology maps alone can already provide significant information on the spatio-temporal heterogeneity of phytoplankton biomass for a specific region. Yoo et al. (2008) compiled eight years of SeaWiFS Chl data to examine seasonal, inter-annual and event-scale variation in phytoplankton in the North Pacific Ocean. They found that the seasonal progression of the timing of the annual Chl peak showed a different pattern when compared with the Atlantic or Indian Ocean, particularly for the North Pacific High Nutrient–Low Chlorophyll (HNLC) regions, which had distinctive autumnal Chl peaks. HNLC regions comprise the eastern equatorial Pacific Ocean, the sub-arctic North Pacific Ocean, and the Southern Ocean. All three regions combined represent a significant portion (30%) of the global oceanic waters and are typically characterized by low spatio-temporal chlorophyll variability with concentrations <0.3 mg m⁻³ (Boyd et al., 2004). However, higher chlorophyll levels can be observed over the generally shallower continental shelves (Tyrrell et al., 2005).

Several phytoplankton bloom detection techniques make use of satellite product climatologies. Some derive concentration thresholds (Park et al., 2010b; Siegel et al., 2002) for a specific region or pixel. Others involve the use of background subtraction methods (Miller et al., 2006; Stumpf et al., 2003) or space–time plots (e.g., Quartly and Srokosz, 2004). Despite being effective techniques for flagging bloom anomalies, possible bias can arise from distorted images that may have been unscreened in the compiled climatology. For instance, the uncorrected influence of the sea bottom in shallow clear waters (Barnes et al., 2013) or the persistence of a bloom for a longer period than the timewindow itself may skew the results obtained from those techniques.

The combined use of several remote sensing products can bring a wealth of information that will help understand the environmental factors that may trigger the onset or the termination of algal bloom events in a specific region (Figs. 10 and 11). Satellite Sea Surface Temperature (SST) data are often used in combination with chlorophyll to relate bloom events to mixed layer depths (Villareal et al., 2012) or upwelling zones (e.g., Thomas et al., 2012; Shi and Wang, 2007). In many cases, however, the sole addition of SST does not suffice; Peñaflores et al. (2007) examined the timing and position of a recurrent, seasonal phytoplankton bloom in the Luzon Strait off the Philippines. Using MODIS Chl and SST, in addition to QuickSCAT wind data and bathymetry, they investigated the possible driving forces behind the bloom occurrence. Their study revealed a complex physical–biological interaction for this area and concluded that high phytoplankton biomass resulted from a combination of intense currents, winds and, possibly, freshwater inputs from nearby rivers, rather than upwelling alone, as previously thought. Other recent studies were unable to detect any long-term trend that could characterize phytoplankton dynamics in the world's oceans from the analysis of global, decadal, multi-source ocean color satellite datasets. Martinez et al. (2009) used global Chl datasets from CZCS and SeaWiFS between 1979 and 2002 and concluded that multidecadal Chl changes appear to be related to “basin-scale oscillations in the physical environment. These oscillations can alternately weaken or emphasize the possible effects

of global warming, making difficult the identification of trends over short time series” (p. 1254). Some studies reported an increase in the magnitude of phytoplankton blooms at a regional (e.g., Kahru and Mitchell, 2008; Richardson and Schoemann, 2004) or global scale (Antoine et al., 2005), whereas others claimed an overall long-term decline in phytoplankton abundance (e.g., Boyce et al., 2010). The latest development in this research is the detection and monitoring of ocean phytoplankton bloom seasonality or phenology (e.g., Demarcq et al., 2012; Racault et al., 2012; Kahru et al., 2010). An example of phytoplankton bloom phenology at a global scale derived from 10 years of SeaWiFS data is shown in Fig. 12.

Data assimilation can be used either for parameter optimization or for state, or flux, estimation. In the context of remote sensing, data assimilation often refers to satellite data being combined with ecosystem models. Zhao et al. (2009a) used several satellite products along with modeled surface current data and geostrophic velocities to explain the occurrence of a near-shore and an offshore phytoplankton bloom in the China Sea following a typhoon. The use of these complementary datasets helped the authors conclude that the near-shore bloom event was induced by terrestrial inputs, whereas the offshore bloom event was triggered by wind-induced upwelling of nutrients. Because ocean color data provide information about water quality variables only (i.e., Chl, TSM, CDOM), they may be limited in their ability to constrain some ecosystem model parameters. This limitation, however, is offset by the volume of data available, covering the full range of biogeochemical responses to the widely varying physical conditions (e.g., Kidston et al., 2013; Wan et al., 2013). Fully operational algal bloom prediction systems using satellite–ecosystem model data assimilation do exist (e.g., the NOAA Harmful Algal Bloom Operational Forecast System (HAB-OFS) for the Gulf of Mexico). Carvalho et al. (2011) provided a comparison study that reported on the sensitivity and effectiveness of empirical (e.g., Anderson et al., 2011), bio-optical (Cannizzaro et al., 2008) and operational (e.g., Banks et al. (2012)) methods to detect HAB. The operational method was found to have an elevated frequency of false-negative cases, whereas both the empirical and bio-optical approaches performed similarly, being equally specific and sensitive.

6. Conclusions and future directions

We have shown that a wide variety of operational ocean color algorithms currently exist to assist in the detection of phytoplankton blooms in most ocean and coastal regions. For simplistic approaches, such as the sole use of the reflectance spectrum, it is recommended that knowledge of the study area and a further detailed analysis of the pixels' reflectance spectra are taken into account to ensure the validity of the algal bloom information retrieved. Band-ratio algorithms are shown to be adequate for open ocean waters, but their use in complex coastal waters is limited, particularly when band-ratios use blue and green bands because the influence of CDOM and TSM at those wavelengths affects their retrievals. Alternatively, many studies have shown the great potential of band-ratios using red and NIR bands to detect Chl-a and algal blooms in coastal waters (e.g., Le et al., 2013) because this spectral region is less affected by those two optically active constituents. Spectral band difference ocean color indices have also been shown to provide reliable information on algal blooms in both open and coastal ocean waters. Ocean color indices are often used in combination with other descriptors to enhance the interpretation of satellite imagery that possibly features algal bloom events (e.g., Yuan et al., 2005). The MERIS MCI in particular is “a versatile tool” (Binding et al., 2012, 2013), but the FLH and FAI, as well as other indices, can be used in conjunction with satellite estimates of Chl-a and SST to improve our image analysis in a very efficient way.

Significant progress has been made in the use and parameterization of bio-optical models in coastal waters, with a new tendency towards using specific inherent optical properties for the detection of phytoplankton blooms instead of the historically used Chl-a proxy (e.g., Tiwari and Shanmugam, 2013). Assessing the accuracy of bio-optical algorithms for the detection, mapping and monitoring of phytoplankton blooms in coastal waters is a prerequisite for the future. There are currently few optical and biogeochemical *in situ* data characterizing pre- and post-blooms conditions. Automated *in situ* sensors, such as Autonomous Underwater Vehicles (AUV) equipped with bio-optical sensors, may provide a solution (IOCCG Report 11, 2011). In addition to parameters derived from ocean color, today's satellite-derived variables also include Photosynthetic Active Radiations (PAR), wind speed and direction, rainfall, salinity and sea surface height (SSH). These variables can all be combined to provide a more complete assessment of the underlying factors of algal bloom events (e.g., Srokosz et al., 2004; Urquhart et al., 2013). The use of multi-source datasets from *in situ* data, satellite products or ecosystem models and their analysis with statistical methods is a prerequisite for fully understanding algal blooms' onset mechanisms and dynamics.

Looking back to the potential of ocean color remote sensing, Cracknell et al. (2001) noted that “*operational real-time monitoring of the location, extent, movement and growth rate of a phytoplankton bloom is an important challenge at present*” (p. 221). The capabilities of ocean color remote sensing in providing operational real-time monitoring of a phytoplankton bloom are progressing but continue to remain a challenge in coastal waters (e.g., Malone, 2008). Coastal ocean covers less than 10% of the global ocean surface but accounts for approximately one third of all marine biological productivity (e.g., Burke et al., 2001). As Siegel et al. (2013) reminded the ocean color community, the future of remote sensing lies in our ability to plan beyond a single sensor mission and to maintain long-term, high-quality, traceable satellite reflectance measurements with sensors' vicarious calibrations, which will make the use of reliable multi-decadal datasets possible. Future satellite instruments and missions should work towards coordinated global coverage of the oceans. Common sets of spectral bands among sensors and a tighter coupling between missions, calibration and validation exercises are desirable (IOCCG Report 13, 2012b). Ocean color satellite mission requirements must be re-evaluated and take into account aspects other than the instrument itself, such as common data processing (e.g., software packages) and management (e.g., centralized data portals). More specifically related to algal blooms, the objectives of future missions are to provide accurate monitoring of HAB, algal bloom timings and magnitudes in optically complex coastal waters, together with the assimilation of satellite-retrieved phytoplankton size or taxa into biogeochemical ecosystem models (e.g., Brewin et al., 2012).

Remote sensing ocean color imagery has provided, and still provides, an invaluable source of frequent, synoptic information. Combined satellite datasets from SeaWiFS, MERIS and MODIS ocean color sensors are equivalent to almost two decades of ocean color imagery for the open and coastal ocean from 1997 to the present, with a brief window of earlier data provided by CZCS from 1979 to 1986. The result is an unprecedented global time series of satellite-derived parameters relevant to algal bloom studies. These ocean color datasets allow for the derivation of ecological baselines, which can then be used to detect and anticipate changes in the ocean system's dynamics (e.g., Siegel et al., 2013; Wong et al., 2009; Smetacek and Cloern, 2008). In addition, archived earth observation data can be used in hindsight to assess prevailing bloom conditions and to identify the biological and physical parameters (e.g., Kahru et al., 1993) that triggered or terminated an algal event. New missions are often delayed, lost, or cancelled, which results in devastating consequences that likely generate satellite

data gaps, such as the 10-year gap between CZCS and SeaWiFS (Fig. 4). This lack of data affected the possibility of answering many environmental questions, one of which was whether the volcanic eruption of Mount Pinatubo in the Philippines in 1991 caused large phytoplankton blooms. The 10 cubic kilometers of material ejected by Mount Pinatubo contained trace metals (Gabrielli et al., 2008), especially iron, that were spread by the winds over the world's oceans. These atmospheric depositions are likely to have generated large-scale phytoplankton blooms, but no ocean color satellite records for those events exist.

Hyperspectral ocean color sensors (Chang et al., 2004) have larger sets of wavelengths that can be used for a more detailed analysis of a remotely sensed signal, whether for chlorophyll retrievals or for the determination of phytoplankton taxa (e.g., Craig et al., 2012; Torrecilla et al., 2011). Geostationary imagers are the new generation of ocean color sensors (IOCCG Report 12, 2012a). By providing ocean color images for a single region several times a day, datasets from geostationary satellites can help resolve the effects of tides and wind events on coastal currents, which are harder to capture with satellite sensors with a daily repeat cycle. The Geostationary Ocean Color Imager (GOCI), the world's first geostationary orbit satellite, was launched in June 27, 2010, acquiring its first image on July 13, 2010. GOCI is designed to monitor the ocean color around the Korean Peninsula with a spatial resolution of 500 m and a temporal resolution of eight images per day.

It is reasonable to predict that hyperspectral satellite sensors with a full set of spectral bands and higher spectral and temporal resolutions (e.g., Lou and Hu, 2014) will enable the development of effective ocean color algorithms and detection schemes for detecting and monitoring phytoplankton blooms in the open and coastal ocean.

Acknowledgments

This research was supported by the combination of three funding sources: a PhD scholarship from the International Postgraduate Research Scholarships (The University of Queensland), a top-up scholarship from the Wealth from Oceans National Research Flagship Program (CSIRO) and The North Australian Marine Research Alliance (NAMRA) post-doctoral Fellowship. The authors are grateful to Mrs. Sandra Edgar-Grant (Charles Darwin University), Dr Ian Leiper (Charles Darwin University) and Elsevier's English Language Editing Service for providing editing support for this manuscript. We would like to thank the space agencies ESA and NASA for providing the satellite images used in this review and the two anonymous reviewers, whose comments significantly improved the paper.

References

- Abbott, M.R., Letelier, R., 1999. MODIS Product Mod-20 Chlorophyll Fluorescence. College of Oceanic and Atmospheric Sciences, Oregon State University, Corvallis, Oregon (USA), p. 42.
- Acker, J. et al., 2008. Remotely-sensed chlorophyll a observations of the northern red sea indicate seasonal variability and influence of coastal reefs. *Journal of Marine Systems* 69, 191–204.
- Ackleson, S.G. et al., 1994. Response of water-leaving radiance to particulate calcite and chlorophyll-a concentrations: a model for gulf of maine coccolithophore blooms. *Journal of Geophysical Research* 99, 7483–7499.
- Ahn, Y.H., Shanmugam, P., 2006. Detecting the red tide algal blooms from satellite ocean color observations in optically complex Northeast-Asia coastal waters. *Remote Sensing of Environment* 103, 419–437.
- Ahn, Y.-H. et al., 2005. Spatial and temporal aspects of phytoplankton blooms in complex ecosystems off the Korean coast from satellite ocean color observations. *Ocean Science Journal* 40, 67–71.
- Ahn, Y.-H. et al., 2006. Satellite detection of harmful algal bloom occurrences in Korean waters. *Harmful Algae* 5, 213–231.
- Aiken, J., Hardman-Mountford, N.J., Barlow, R., Fishwick, J., Hirata, T., Smyth, T., 2008. Functional links between bioenergetics and bio-optical traits of phytoplankton taxonomic groups: an overarching hypothesis with applications for ocean colour remote sensing. *Journal of Plankton Research* 30 (2), 165–181.

- Amin, R. et al., 2008. Detection of *Karenia brevis* Harmful Algal Blooms in the West Florida Shelf Using Red Bands of MERIS Imagery. IEEE OCEANS 2008. IEEE, Quebec, Canada.
- Amin, R. et al., 2009a. MODIS and MERIS detection of dinoflagellate blooms using the Rbd technique. In: 2009 Conference on Remote Sensing of the Ocean, Sea Ice, and Large Water Regions. Berliner Congress Centre, Berlin: SPIE.
- Amin, R. et al., 2009b. Novel optical techniques for detecting and classifying toxic dinoflagellate *Karenia brevis* blooms using satellite imagery. Optics Express 17, 9126–9144.
- Anderson, C.R. et al., 2011. Detecting toxic diatom blooms from ocean color and a regional ocean model. Geophysical Research Letters 38 (4), L04603.
- Antoine, D. et al., 2005. Bridging ocean color observations of the 1980s and 2000s in search of long-term trends. Journal of Geophysical Research 110 (C6).
- Babin, M. et al., 2003. Variations in the light absorption coefficients of phytoplankton, nonalgal particles, and dissolved organic matter in coastal waters around Europe. Journal of Geophysical Research 108 (C7).
- Babin, S.M. et al., 2004. Satellite evidence of hurricane-induced phytoplankton blooms in an oceanic desert. Journal of Geophysical Research 109 (C03043).
- Babin, M. et al., 2008. Real-Time Coastal Observing Systems for Marine Ecosystem Dynamics and Harmful Algal Blooms: Theory, Instrumentation and Modelling. UNESCO, Paris.
- Balch, W.M. et al., 2005. Calcium carbonate measurements in the surface global ocean based on moderate-resolution imaging spectroradiometer data. Journal of Geophysical Research 110, 1–21.
- Banks, A.C. et al., 2012. A satellite ocean color observation operator system for eutrophication assessment in coastal waters. Journal of Marine Systems 94 (Suppl.), S2–S15.
- Banse, K., English, D.C., 1994. Seasonality of coastal zone color scanner phytoplankton pigment in the offshore oceans. Journal of Geophysical Research 99, 7323–7345.
- Banse, K., English, D.C., 1997. Near-surface phytoplankton pigment from the coastal zone color scanner in the subantarctic region southeast of New Zealand. Marine Ecology Progress Series 156, 51–66.
- Banse, K., English, D.C., 1999. Comparing phytoplankton seasonality in the eastern and western subarctic Pacific and the western Bering Sea. Progress in Oceanography 43, 235–288.
- Banse, K., English, D.C., 2000. Geographical differences in seasonality of CZCS-derived phytoplankton pigment in the Arabian Sea for 1978–1986. Deep Sea Research 47, 1623–1677.
- Barnes, B.B. et al., 2013. MODIS-derived spatio-temporal water clarity patterns in optically shallow Florida keys waters: a new approach to remove bottom contamination. Remote Sensing of Environment 134, 377–391.
- Behrenfeld, M.J. et al., 2009. Satellite-detected fluorescence reveals global physiology of ocean phytoplankton. Biogeosciences 6, 779–794.
- Bergamino, N. et al., 2010. Spatio-temporal dynamics of phytoplankton and primary production in Lake Tanganyika using a MODIS based bio-optical time series. Remote Sensing of Environment 114, 772–780.
- Bernard, S. et al., 2005. The use of MERIS for harmful algal bloom monitoring in the Southern Benguela. In: Lacoste, H. (Ed.), MAVT, vol. 348. ESRIN, Frascati (It.), pp. 1–7.
- Bierman, P. et al., 2011. A review of methods for analysing spatial and temporal patterns in coastal water quality. Ecological Indicators 11, 103–114.
- Binding, C.E. et al., 2012. The MERISMc and its potential for satellite detection of winter diatom blooms on partially ice-covered Lake Erie. Journal of Plankton Research 34, 569–573.
- Binding, C.E. et al., 2013. The MERIS maximum chlorophyll index; its merits and limitations for inland water algal bloom monitoring. Journal of Great Lakes Research.
- Blondeau-Patissier, D., 2011. Detection and Quantification of Algal Bloom Dynamics in the Great Barrier Reef Lagoonal Waters Using Remote Sensing and Bio-Optics. School of Geography, Planning and Environmental Management. University of Queensland, Brisbane, p. 334.
- Blondeau-Patissier, D. et al., 2004. Comparison of bio-physical marine products from SeaWiFS, MODIS and a bio-optical model with in situ measurements from Northern European waters. Journal of Optics A: Pure and Applied Optics 6, 875–889.
- Blondeau-Patissier, D. et al., 2009. Bio-optical variability of the absorption and scattering properties of the Queensland inshore and reef waters, Australia. Journal of Geophysical Research 114 (C05003).
- Bostater Jr., C.R. et al., 2003. Hyperspectral remote sensing protocol development for submerged aquatic vegetation in shallow waters. In: Bostater, C.R., Jr., Santoleri, R. (Eds.), Remote Sensing of the Ocean and Sea Ice, vol. 5233. SPIE, Barcelona, Spain, pp. 199–215.
- Bowers, D.G. et al., 1996. Absorption spectra of inorganic particles in the Irish Sea and their relevance to remote sensing of chlorophyll. International Journal of Remote Sensing 17, 2449–2460.
- Boyce, D.G. et al., 2010. Global phytoplankton decline over the past century. Nature 466, 591–596.
- Boyd, P.W. et al., 2004. Episodic enhancement of phytoplankton stocks in New Zealand subantarctic waters: contribution of atmospheric and oceanic iron supply. Global Biogeochemical Cycles 18, GB1029.
- Brando, V.E. et al., 2012. An adaptive semi-analytical inversion of ocean colour radiometry in optically complex waters. Applied Optics 51, 2808–2833.
- Brewin, R.J.W. et al., 2011. An intercomparison of bio-optical techniques for detecting dominant phytoplankton size class from satellite remote sensing. Remote Sensing of Environment 115, 325–339.
- Brewin, R.J.W. et al., 2012. The influence of the Indian Ocean dipole on interannual variations in phytoplankton Size Structure as revealed by earth observation. Deep-Sea Research Part II: Topical Studies in Oceanography 77–80, 117–127.
- Brewin, R.J.W., Raitsos, D.E., Pradhan, Y., Hoteit, I., 2013. Comparison of chlorophyll in the Red Sea derived from MODIS-Aqua and in vivo fluorescence. Remote Sensing of Environment 136, 218–224.
- Briand, A., Claustré, H., Ras, J., Oubelkheir, K., 2004. Natural variability of phytoplanktonic absorption in oceanic waters: influence of the size structure of algal populations. Journal of Geophysical Research 109, C11010.
- Brickley, P.J., Thomas, A.C., 2004. Satellite-measured seasonal and inter-annual chlorophyll variability in the Northeast Pacific and coastal Gulf of Alaska. Deep Sea Research Part II: Topical Studies in Oceanography 51, 229–245.
- Brody, S.R., Lozier, M.S., Dunne, J.P., 2013. A comparison of methods to determine phytoplankton bloom initiation. Journal of Geophysical Research: Oceans 118 (5), 2345–2357.
- Brown, C.W., 1995. Global distribution of coccolithophore blooms. Oceanography 8, 59–60.
- Brown, C.W., Podesta, G.P., 1997. Remote sensing of coccolithophore blooms in the western South Atlantic ocean. Remote Sensing of Environment 60, 83–91.
- Brown, C.W., Yoder, J.A., 1994a. Coccolithophorid blooms in the global ocean. Journal of Geophysical Research 99, 7467–7482.
- Brown, C.W., Yoder, J.A., 1994b. Distribution pattern of coccolithophorid blooms in the western North Atlantic Ocean. Continental Shelf Research 14, 175–197.
- Burke, L.A. et al., 2001. Pilot Analysis of Global Ecosystems: Coastal Ecosystems. World Resources Institute, Washington, DC, p. 94.
- Campbell, J.W., Feng, H., 2005a. The Empirical Chlorophyll Algorithm for MODIS: Testing the Oc3m Algorithm Using Nomad Data. Ocean Color Bio-optical Algorithm Mini Workshop (OCBAM). University of New Hampshire, Durham (USA): Ocean Color Bio-optical Algorithm Mini Workshop (OCBAM).
- Campbell, J.W., Feng, H., 2005b. The Empirical Chlorophyll Algorithm for SeaWiFS: Testing the Oc4.V4 Algorithm Using Nomad Data Ocean Color Bio-optical Algorithm Mini Workshop (OCBAM). University of New Hampshire, Durham (USA).
- Cannizzaro, J., 2004. Detection and Quantification of *Karenia brevis* Blooms on the West Florida Shelf from Remotely Sensed Ocean Color Imagery Vol. MSc College of Marine Science, University of South Florida, p. 81.
- Cannizzaro, J.P. et al., 2008. A novel technique for detection of the toxic dinoflagellate, *Karenia brevis*, in the Gulf of Mexico from remotely sensed ocean color data. Continental Shelf Research 28, 137–158.
- Carvalho, G.A. et al., 2010. Satellite remote sensing of harmful algal blooms: a new multi-algorithm method for detecting the Florida red tide (*Karenia brevis*). Harmful Algae 9, 440–448.
- Carvalho, G.A. et al., 2011. Long-term evaluation of three satellite ocean color algorithms for identifying harmful algal blooms (*Karenia brevis*) along the west coast of Florida: a matchup assessment. Remote Sensing of Environment 115, 1–18.
- Chang, N.B., Xuan, Z.M., 2011. Exploring the nutrient inputs and cycles in Tampa Bay and coastal watersheds using MODIS images and data mining. In: Gao, W. et al. (Eds.), Remote Sensing and Modeling of Ecosystems for Sustainability VIII, vol. 8156. Spie-IntSoc Optical Engineering, Bellingham.
- Chang, G. et al., 2004. The new age of hyperspectral oceanography. Oceanography, 23–29.
- Chari, N.V.H.K. et al., 2013. Fluorescence and absorption characteristics of dissolved organic matter excreted by phytoplankton species of Western Bay of Bengal under Axenic Laboratory condition. Journal of Experimental Marine Biology and Ecology 445, 148–155.
- Chen, J., Quan, W., 2013. An improved algorithm for retrieving chlorophyll-a from the yellow river estuary using MODIS imagery. Environmental Monitoring and Assessment 185, 2243–2255.
- Claustre, H., Maritorena, S., 2003. The many shades of ocean blue. Science 302, 1514–1515.
- Claustre, H., Babin, M., Merien, D., Ras, J., Prieur, L., Dallot, S., Prasil, O., Dousova, H., Moutin, T., 2005. Toward a taxon-specific parameterization of bio-optical models of primary production: a case study in the North Atlantic.. Journal of Geophysical Research 110, C07S12.
- Cracknell, A.P. et al., 2001. The Abdmap (algal bloom detection, monitoring and prediction) concerted action. International Journal of Remote Sensing 22, 205–247.
- Craig, S.E. et al., 2012. Deriving optical metrics of coastal phytoplankton biomass from ocean colour. Remote Sensing of Environment 119, 72–83.
- Cullen, J.J., 1982. The deep chlorophyll maximum: comparing vertical profiles of chlorophyll-A. Canadian Journal of Fisheries and Aquatic Sciences 39, 791–803.
- Dasgupta, S. et al., 2009. Comparison of global chlorophyll concentrations using MODIS data. Advances in Space Research 43, 1090–1100.
- Demarcq, H. et al., 2012. Monitoring marine phytoplankton seasonality from space. Remote Sensing of Environment 117, 211–222.
- Dickey, T. et al., 2006. Optical oceanography: recent advances and future directions using global remote sensing and in situ observations. Reviews of geophysics 44, RG1001.
- Dierssen, H.M., 2010. Perspectives on empirical approaches for ocean color remote sensing of chlorophyll in a changing climate. Proceeding of the National Academy of Sciences of the United States of America 107, 17073–17078.
- Dierssen, H.M., Smith, R.C., 2000. Bio-optical properties and remote sensing ocean color algorithms for Antarctic Peninsula waters. Journal of Geophysical Research 105, 26301–26312.

- Dierssen, H.M. et al., 2006. Red and black tides: quantitative analysis of water-leaving radiance and perceived color for phytoplankton, colored dissolved organic matter, and suspended sediments. *Limnology and Oceanography* 51, 2646–2659.
- Dierssen, H.M. et al., 2007. The Red Edge: Exploring High Near-Infrared Reflectance of Phytoplankton and Submerged Macrophytes and Implications for Aquatic Remote Sensing. AGU Spring Meeting 2007: American Geophysical Union.
- Dore, J.E., Letelier, R.M., Church, M.J., Lukas, R., Karl, D.M., 2008. Summer phytoplankton blooms in the oligotrophic North Pacific Subtropical Gyre: historical perspective and recent observations. *Progress in Oceanography* 76 (1), 2–38.
- Dupouy, C. et al., 2008. Bio-optical properties of the marine cyanobacteria *Trichodesmium* spp. *Journal of Applied Remote Sensing* 2 (1), 023503.
- Dupouy, C. et al., 2011. An algorithm for detecting *Trichodesmium* surface blooms in the south western tropical Pacific. *Biogeosciences Discussions* 8, 5653–5689.
- Falkowski, P., Kiefer, D.A., 1985. Chlorophyll-a fluorescence in phytoplankton: relationship to photosynthesis and biomass. *Journal of Plankton Research* 7, 715–731.
- Fargion, G.S., McClain, C.R., 2003. An Overview of SIMBIOS Program Activities and Accomplishments. SIMBIOS Project; 2003 Annual Report. NASA Goddard Space Flight Center, Greenbelt (Maryland, USA), pp. 1–33.
- Feldman, G. et al., 1984. Satellite color observations of the phytoplankton distribution in the eastern equatorial Pacific during the 1982–1983 El Niño. *Science* 226, 1069–1071.
- Focardi, S. et al., 2009. A combined approach to investigate the biochemistry and hydrography of a shallow bay in the South Adriatic Sea: the Gulf of Manfredonia (Italy). *Environmental Monitoring and Assessment* 153, 209–220.
- Franz, B., Kwiatowska, E.J., Meister, G., McClain, C.R., 2008. Moderate resolution imaging spectroradiometer on Terra: limitations for ocean color applications. *Journal of Applied Remote Sensing* 2 (1).
- Frolov, S. et al., 2013. Monitoring of harmful algal blooms in the era of diminishing resources: a case study of the U.S. West Coast. *Harmful Algae* 21–22, 1–12.
- Fuentes-Yaco, C. et al., 1997a. Phytoplankton pigment in the Gulf of St. Lawrence, Canada, as determined by the coastal zone color scanner – Part Ii: Multivariate Analysis. *Continental Shelf Research* 17, 1441–1459.
- Fuentes-Yaco, C. et al., 1997b. Phytoplankton pigment in the Gulf of St. Lawrence, Canada, as determined by the coastal zone color scanner – Part I: Spatio-temporal variability. *Continental Shelf Research* 17, 1421–1439.
- Gabric, A.J. et al., 1990. Spatio-temporal variability in surface chlorophyll distribution in the central Great Barrier Reef as derived from CZCS imagery. *Australian Journal of Marine and Freshwater Research* 41, 313–324.
- Gabrielli, P. et al., 2008. Siderophile metal fallout to Greenland from the 1991 winter eruption of Hekla (Iceland) and during the global atmospheric perturbation of Pinatubo. *Chemical Geology* 255, 78–86.
- Garcia, C.A.E., Garcia, V.M.T., 2008. Variability of chlorophyll-a from ocean color images in the La Plata continental shelf region. *Continental Shelf Research* 28, 1568–1578.
- Garcia, R. et al., 2013. Quantification of Floating Macroalgae Blooms Using the Scaled Algae Index (Sai). *Journal of Great Lakes Research* 118, 26–46.
- Garcia-Soto, C., Pingree, R.D., 2009. Spring and summer blooms of phytoplankton (SeaWiFS/MODIS) along a ferry line in the Bay of Biscay and western English Channel. *Continental Shelf Research* 29, 1111–1122.
- Garver, S.A., Siegel, D.A., 1997. Inherent optical property inversion of ocean color spectra and its biogeochemical interpretation – 1. Time series from the Sargasso Sea. *Journal of Geophysical Research* 102, 18607–18625.
- Gazeau, F., Smith, S.V., Gentili, B., Frankignoulle, M., Gattuso, J.-P., 2004. The European coastal zone: characterization and first assessment of ecosystem metabolism. *Estuarine, Coastal and Shelf Science* 60 (4), 673–694.
- Gilerson, A. et al., 2007. Fluorescence component in the reflectance spectra from coastal waters. I. Dependence on water composition. *Optics Express* 15, 15702–15721.
- Gilerson, A. et al., 2008. Fluorescence component in the reflectance spectra from coastal waters. II. Performance of retrieval algorithms. *Optics Express* 16, 2446–2460.
- Gitelson, A., 1992. The peak near 700 nm on radiance spectra of algae and water: relationships of its magnitude and position with chlorophyll concentration. *International Journal of Remote Sensing* 13, 3367–3373.
- Gitelson, A. et al., 1999. Comparative reflectance properties of algae cultures with manipulated densities. *Journal of Applied Phycology* 11, 345–354.
- Gitelson, A.A. et al., 2009. A bio-optical algorithm for the remote estimation of the chlorophyll-a concentration in case 2 waters. *Environmental Research Letters* 4, 5.
- Goela, P.C. et al., 2013. Specific absorption coefficient of phytoplankton off the southwest coast of the Iberian Peninsula: a contribution to algorithm development for ocean colour remote sensing. *Continental Shelf Research* 52, 119–132.
- Gohin, F. et al., 2003. Satellite and in situ observations of a late winter phytoplankton bloom, in the Northern Bay of Biscay. *Continental Shelf Research* 23, 1117–1141.
- Gordoa, A. et al., 2008. Spatio-temporal patterns in the North-Western Mediterranean from MERIS derived chlorophyll-a concentration. *Scientia Marina* 72, 757–767.
- Gordon, H.R. et al., 1980. Phytoplankton pigments from the Nimbus-7 coastal zone color scanner: comparisons with surface measurements. *Science* 210, 63–66.
- Gordon, H.R. et al., 1983. Phytoplankton pigment concentrations in the Middle Atlantic Bight: comparison of ship determinations and coastal zone color scanner measurements. *Applied Optics* 22, 4175–4180.
- Gower, J., 2000. Productivity and plankton blooms observed with SeaWiFS. In: Proceedings of the Fifth Pacific Ocean Remote Sensing Conference (Porsec), 5–8 December 2000, vol. 1. NIO Dona Paula Goa (India), pp. 23–27.
- Gower, J., 2001. Productivity and plankton blooms observed with SeaWiFS and in situ sensors. *IEEE Geoscience and Remote Sensing Letters* 5, 2181–2183.
- Gower, J., Borstad, G.A., 2004. On the potential of MODIS and MERIS for imaging chlorophyll fluorescence from space. *International Journal of Remote Sensing* 25, 1459–1464.
- Gower, J., King, S., 2007a. An Antarctic ice-related “superbloom” observed with the MERIS satellite imager. *Geophysical Research Letters*, 34.
- Gower, J., King, S., 2007b. Validation of chlorophyll fluorescence derived from MERIS on the west coast of Canada. *International Journal of Remote Sensing* 28, 625–635.
- Gower, J., King, S., 2008. Satellite Images Show the Movement of Floating *Sargassum* in the Gulf of Mexico and Atlantic Ocean. *Nature Proceedings*.
- Gower, J., King, S., 2011a. A global survey of intense surface plankton blooms and floating vegetation using MERIS MCI. In: Tang, D. (Ed.), *Remote Sensing of the Changing Oceans*. Springer, p. 396.
- Gower, J., King, S.A., 2011b. Distribution of floating *Sargassum* in the Gulf of Mexico and the Atlantic Ocean mapped using MERIS. *International Journal of Remote Sensing* 32, 1917–1929.
- Gower, J. et al., 1999. Interpretation of the 685 nm peak in water-leaving radiance spectra in terms of fluorescence, absorption and scattering, and its observation by MERIS. *International Journal of Remote Sensing* 20, 1771–1786.
- Gower, J. et al., 2003. Use of 709 nm band of MERIS to detect intense plankton blooms and other conditions in coastal waters. In: ESA (Ed.), *MERIS User Workshop*. ESA, Frascati (It.), p. 6.
- Gower, J. et al., 2004. Observation of chlorophyll fluorescence in west coast waters of Canada using the MODIS satellite sensor. *Canadian Journal of Remote Sensing* 30, 17–25.
- Gower, J. et al., 2005. Detection of intense plankton blooms using the 709 nm band of the MERIS imaging spectrometer. *International Journal of Remote Sensing* 26, 2005–2012.
- Gower, J. et al., 2006. Ocean color satellites show extensive lines of floating *Sargassum* in the Gulf of Mexico. *IEEE Transaction on Geoscience and Remote Sensing* 44, 3619–3625. <http://dx.doi.org/10.1109/TGRS.2006.882258>.
- Gower, J. et al., 2008. Global monitoring of plankton blooms using MERIS MCI. *International Journal of Remote Sensing* 29, 21.
- Gower, J., Young, E., King, S., 2013. Satellite images suggest a new *Sargassum* source region in 2011. *Remote Sensing Letters* 4 (8), 764–773.
- Gurlin, D. et al., 2011. Remote estimation of chl-a concentration in turbid productive waters: return to a simple two-band NIR-red model? *Remote Sensing of Environment* 115, 3479–3490.
- Hardman-Mountford, N.J. et al., 2008. An objective methodology for the classification of ecological pattern into biomes and provinces for the pelagic ocean. *Remote Sensing of Environment* 112, 3341–3352.
- Harley, J. et al., 2011. Biogeochemical study of a coccolithophore bloom in the Northern Bay of Biscay (Ne Atlantic Ocean) in June 2004. *Progress in Oceanography* 86, 317–336.
- Hegseth, E.N., Sundfjord, A., 2008. Intrusion and blooming of Atlantic phytoplankton species in the high arctic. *Journal of Marine Systems* 74, 108–119.
- Henson, S.A., Thomas, A.C., 2007. Interannual variability in timing of bloom initiation in the California current system. *Journal of Geophysical Research* 112, C8.
- Henson, S.A. et al., 2006. Effect of meteorological conditions on interannual variability in timing and magnitude of the spring bloom in the Irminger Basin, North Atlantic. *Deep Sea Research (Part I)* 53, 1601–1615.
- Henson, S.A. et al., 2009. Decadal variability in north Atlantic phytoplankton blooms. *Journal of Geophysical Research C: Oceans* 114, C04013.
- Hoge, F.E. et al., 2003. Validation of terra-MODIS phytoplankton chlorophyll fluorescence line height. I. Initial airborne lidar results. *Applied Optics* 42 (15).
- Holligan, P.M. et al., 1983. Satellite and ship studies of coccolithophore production along a continental shelf edge. *Nature* 304, 339–342.
- Holligan, P.M. et al., 2010. Seasonal distributions of the coccolithophore, *Emiliania huxleyi*, and of particulate inorganic carbon in surface waters of the Scotia Sea. *Journal of Marine Systems* 82, 195–205.
- Hu, C., 2009. A novel ocean color index to detect floating algae in the global oceans. *Remote Sensing of Environment* 113, 2118–2129.
- Hu, C. et al., 2000. How precise are SeaWiFS ocean color estimates? Implications of digitization-noise errors. *Remote Sensing of Environment* 76, 239–249.
- Hu, C. et al., 2004. Linkages between coastal runoff and the Florida Keys ecosystem: a study of a Dark Plume event. *Geophysical Research Letters* 31, L15307.
- Hu, C. et al., 2005. Red tide detection and tracing using MODIS fluorescence data: a regional example in SW Florida coastal waters. *Remote Sensing of Environment* 97, 311–321.
- Hu, C. et al., 2010a. Remote detection of *Trichodesmium* blooms in optically complex coastal waters: examples with MODIS full-spectral data. *Remote Sensing of Environment* 114, 2048–2058.
- Hu, C. et al., 2010b. On the recurrent *Ulva prolifera* blooms in the yellow sea and East China Sea. *Journal of Geophysical Research* 115, C05017.
- Hu, C. et al., 2010c. Moderate Resolution Imaging Spectroradiometer (MODIS) observations of cyanobacteria blooms in Taihu Lake, China. *Journal of Geophysical Research-Oceans* 115, C04002.

- Hu, C. et al., 2012. Chlorophyll a algorithms for oligotrophic oceans: a novel approach based on three-band reflectance difference. *Journal of Geophysical Research* 117 (C1), C01011.
- Huang, N.E. et al., 1998. The Empirical Mode Decomposition and the Hilbert Spectrum for Nonlinear and Non-Stationary Time Series Analysis. Royal Society of London, vol. 454. London, pp. 903–995.
- Huisman, J., Pham Thi, N.N., Karl, D.M., Sommeijer, B., 2006. Reduced mixing generates oscillations and chaos in the oceanic deep chlorophyll maximum. *Nature* 439 (7074), 322–325.
- Iida, T., Saitoh, S.-I., 2007. Temporal and spatial variability of chlorophyll concentrations in the Bering Sea using empirical orthogonal function (Eof) analysis of remote sensing data. *Deep Sea Research Part II: Topical Studies in Oceanography* 54, 2657–2671.
- Iida, T. et al., 2002. Temporal and spatial variability of coccolithophore blooms in the eastern Bering Sea, 1998–2001. *Progress in Oceanography* 55, 165–175.
- Iida, T. et al., 2012. Interannual variability of coccolithophore *Emiliania huxleyi* blooms in response to changes in water column stability in the eastern Bering Sea. *Continental Shelf Research* 34, 7–17.
- IOCCG, 2008. Why ocean colour? The societal benefits of ocean-colour technology. In: Platt, T. et al. (Eds.), Reports of the International Ocean-Colour Coordinating Group. Bedford Institute, Dartmouth (Nova Scotia, Ca.).
- IOCCG, 2009. Partition of the ocean into ecological provinces: role of ocean-colour radiometry. In: Dowell, M., Platt, T. (Eds.), Reports of the International Ocean-Colour Coordinating Group. Bedford Institute, Dartmouth (Nova Scotia, Ca.).
- IOCCG, 2011. Bio-optical sensors on argo floats. In: Claustre, H. (Ed.), Reports of the International Ocean Colour Coordinating Group. Laboratoire d'Océanographie de Villefranche (LOV-CNRS), Villefranche-sur-mer (Fr.), p. 89.
- IOCCG, 2012a. Ocean-colour observations from a geostationary orbit. In: Antoine, D. (Ed.), Reports of the International Ocean Colour Coordinating Group. Laboratoire d'Océanographie de Villefranche (LOV-CNRS), Villefranche-sur-mer (Fr.), p. 102.
- IOCCG, 2012b. Mission requirements for future ocean-colour sensors. In: McClain, C., Meister, G. (Eds.), Reports of the International Ocean Colour Coordinating Group. NASA Goddard Space Flight Center, Greenbelt (MD, USA), p. 106.
- Jessup, D.A. et al., 2009. Mass stranding of marine birds caused by a surfactant-producing red tide. *PLoS One* 4, 8.
- Joint, I.I., Groom, S.B., 2000. Estimation of phytoplankton production from space: current status and future potential of satellite remote sensing. *Journal of Experimental Marine Biology and Ecology* 250, 233–255.
- Kahru, M., Mitchell, B.G., 2008. Ocean color reveals increased blooms in various parts of the world. *Eos, Transactions, American Geophysical Union* 89, 170.
- Kahru, M. et al., 1993. Cyanobacterial blooms cause heating of the sea surface. *Marine Ecology Progress Series* 101, 1–7.
- Kahru, M. et al., 2004. MODIS detects a devastating algal bloom in paracas bay, Peru. *Eos, Transactions, American Geophysical Union* 85, 465–472.
- Kahru, M. et al., 2010. Are phytoplankton blooms occurring earlier in the Arctic? *Global Change Biology*, 1733–1739.
- Kidston, M., Matear, R., Baird, M.E., 2013. Phytoplankton growth in the Australian sector of the Southern Ocean, examined by optimising ecosystem model parameters. *Journal of Marine Systems* 128, 123–137.
- Kim, S. et al., 2000. Temporal and spatial variability of phytoplankton pigment concentrations in the Japan sea derived from CZCS images. *Journal of Oceanography* 56, 527–538.
- Kitsiou, D., Karydis, M., 2011. Coastal marine eutrophication assessment: a review on data analysis. *Environment International* 37, 778–801.
- Klemas, V., 2011. Remote sensing techniques for studying coastal ecosystems: an overview. *Journal of Coastal Research* 27, 2–17.
- Klemas, V., 2012. Remote sensing of algal blooms: an overview with case studies. *Journal of Coastal Research* 28, 34–43.
- Kogeler, J., Rey, F., 1999. Ocean colour and the spatial and seasonal distribution of phytoplankton in the Barents Sea. *International Journal of Remote Sensing* 20, 1303–1318.
- Komick, N.M. et al., 2009. Bio-optical algorithm evaluation for MODIS for Western Canada coastal waters: an exploratory approach using in situ reflectance. *Remote Sensing of Environment* 113, 794–804.
- Kratzer, S. et al., 2013. The use of ocean color remote sensing in integrated coastal zone management—a case study from Himmerfjärden, Sweden. *Marine Policy*.
- Kurekin, A.A., Miller, P.I., Van der Woerd, H.J., 2014. Satellite discrimination of Karenia mikimotoi and Phaeocystis harmful algal blooms in European coastal waters: merged classification of ocean colour data. *Harmful Algae* 31, 163–176.
- Kutser, T., 2009. Passive optical remote sensing of cyanobacteria and other intense phytoplankton blooms in coastal and inland waters. *International Journal of Remote Sensing* 30, 4401–4425.
- LaRoche, J., Breitbarth, E., 2005. Importance of the diazotrophs as a source of new nitrogen in the ocean. *Journal of Sea Research* 53, 67–91.
- Lavender, S.J., Groom, S.B., 2001. The detection and mapping of algal blooms from space. *International Journal of Remote Sensing* 22, 197–201.
- Le, C. et al., 2013. Towards a long-term chlorophyll-a data record in a turbid estuary using MODIS observations. *Progress in Oceanography* 109, 90–103.
- Lee, Z. et al., 2002. Deriving inherent optical properties from water color: a multiband quasi-analytical algorithm for optically deep waters. *Applied Optics* 41, 5755–5772.
- Lee, Z., Carde, K., Arnone, R., He, M.-X., 2007. Determination of primary spectral bands for remote sensing of aquatic environments. *Sensors* 7 (12), 3428–3441.
- Letelier, R.M., Abbott, M.R., 1996. An analysis of chlorophyll fluorescence algorithms for the moderate resolution imaging spectrometer (MODIS). *Remote Sensing of Environment* 58, 215–223.
- Li, H. et al., 2010a. Enhancing generic ecological model for short-term prediction of Southern North Sea algal dynamics with remote sensing images. *Ecological Modelling* 221, 2435–2446.
- Li, K. et al., 2010b. Spatial-temporal variation of chlorophyll-a concentration in the Bohai Sea. *Lecture Notes in Computer Science* 6330, 662–670.
- Longhurst, A., 1995. Seasonal cycles of pelagic production and consumption. *Progress in Oceanography* 36, 77–167.
- Lou, X., Hu, C., 2014. Diurnal changes of a harmful algal bloom in the East China Sea: observations from GOCE. *Remote Sensing of Environment* 140, 562–572.
- Malone, T.C., 2008. Ecosystem dynamics, harmful algal blooms and operational oceanography. In: Babin, M. et al. (Eds.), Real-Time Coastal Observing Systems for Marine Ecosystem Dynamics and Harmful Algal Blooms: Theory, Instrumentation and Modelling. *Oceanographic Methodology Series*, UNESCO, Paris, pp. 527–560.
- Marinelli, M.A. et al., 2008. A remote sensing study of the phytoplankton spatial-temporal cycle in the Southeastern Indian Ocean. *Journal of Applied Remote Sensing*, 2.
- Maritorena, S. et al., 2002. Optimization of a semianalytical ocean color model for global applications. *Applied Optics* 41, 2705–2714.
- Maritorena, S. et al., 2010. Merged satellite ocean color data products using a bio-optical model: characteristics, benefits and issues. *Remote Sensing of Environment* 114, 1791–1804.
- Marrari, M. et al., 2008. Spatial and temporal variability of SeaWiFS chlorophyll a distributions west of the Antarctic Peninsula: implications for krill production. *Deep-Sea Research Part II* 55, 377–392.
- Martin, A.P., 2003. Phytoplankton patchiness: the role of lateral stirring and mixing. *Progress in Oceanography* 57, 125–174.
- Martinez, E. et al., 2009. Climate-driven basin-scale decadal oscillations of oceanic phytoplankton. *Science* 326, 1253–1256.
- Matthews, M.W., 2011. A current review of empirical procedures of remote sensing in Inland and near-coastal transitional waters. *International Journal of Remote Sensing* 32, 6855–6899.
- Matthews, M.W. et al., 2012. An algorithm for detecting trophic status (chlorophyll-a), cyanobacterial-dominance, surface scums and floating vegetation in Inland and coastal waters. *Remote Sensing of Environment* 124, 637–652.
- McClain, C.R., 2009a. A decade of satellite ocean color observations. *Annual Review of Marine Science* 1, 19–42.
- McClain, C.R., 2009b. Satellite remote sensing: ocean color. In: Steele, J.H. et al. (Eds.), *Encyclopedia of Ocean Sciences*, second ed. Academic Press, Oxford, pp. 114–126.
- McKee, D. et al., 2007. Potential Impacts of non-algal materials on water-leaving sun-induced chlorophyll fluorescence signals in coastal waters. *Applied Optics* 46, 7720–7729.
- McKinna, L.I.W. et al., 2011. A simple, binary classification algorithm for the detection of *Trichodesmium* spp. within the great barrier reef using MODIS imagery. *Limnology and Oceanography-Methods* 9, 50–66.
- Mélin, F. et al., 2011. Multi-sensor satellite time series of optical properties and chlorophyll-a concentration in the Adriatic Sea. *Progress in Oceanography* 91, 229–244.
- Merico, A. et al., 2003. Analysis of satellite imagery for *Emiliania huxleyi* blooms in the Bering Sea before 1997. *Geophysical Research Letters* 30, 1337.
- Miller, P.I. et al., 2006. SeaWiFS discrimination of harmful algal bloom evolution. *International Journal of Remote Sensing* 27, 2287–2301.
- Moore, T.S. et al., 2009. A class-based approach to characterizing and mapping the uncertainty of the MODIS ocean chlorophyll product. *Remote Sensing of Environment* 113, 2424–2430.
- Moore, T.S. et al., 2012. Detection of coccolithophore blooms in ocean color satellite imagery: a generalized approach for use with multiple sensors. *Remote Sensing of Environment* 117, 249–263.
- Morel, A., 1980. In-water and remote measurements of ocean color. *Boundary Layer Meteorology* 18, 177–201.
- Morel, A., 2001. Bio-optical models. In: Steele, J.H. et al. (Eds.), *Encyclopedia of Ocean Sciences*. Academic Press, New York, pp. 317–326.
- Morel, A., Prieur, R., 1977. Analysis of variations in ocean color. *Limnology and Oceanography* 22, 709–722.
- Moses, W.J. et al., 2012. Operational MERIS-based NIR-red algorithms for estimating chlorophyll-a concentrations in coastal waters—the Azov Sea case study. *Remote Sensing of Environment* 121, 118–124.
- Mouw, C.B. et al., 2012. Impact of phytoplankton community size on a linked global ocean optical and ecosystem model. *Journal of Marine Systems* 89, 61–75.
- Navarro, G., Ruiz, J., 2006. Spatial and temporal variability of phytoplankton in the Gulf of Cádiz through remote sensing images. *Deep Sea Research Part II: Topical Studies in Oceanography* 53, 1241–1260.
- Neville, R.A., Gower, J., 1977. Passive remote sensing of phytoplankton via chlorophyll fluorescence. *Journal of Geophysical Research* 82, 3487–3493.
- Nezlin, N.P., Li, B.-L., 2003. Time-series analysis of remote-sensed chlorophyll and environmental factors in the Santo Monica–San Pedro Basin off Southern California. *Journal of Marine Systems* 39, 185–202.
- Nezlin, N.P. et al., 1999. Patterns of seasonal and interannual changes of surface chlorophyll concentration in the black sea revealed from the remote sensed data. *Remote Sensing of Environment* 69, 43–55.

- Nezlin, N.P. et al., 2010. Satellite monitoring of climatic factors regulating phytoplankton variability in the Arabian (Persian) Gulf. *Journal of Marine Systems* 82, 47–60.
- Odermatt, D. et al., 2012. Review of constituent retrieval in optically deep and complex waters from satellite imagery. *Remote Sensing of Environment* 118, 116–126.
- Oliveira, P.B. et al., 2009. Summer diatom and dinoflagellate blooms in Lisbon Bay from 2002 to 2005: pre-conditions inferred from wind and satellite data. *Progress in Oceanography* 83, 270–277.
- Oliver, M.J., Irwin, A.J., 2008. Objective global ocean biogeographic provinces. *Geophysical Research Letters*, 35.
- O'Reilly, J.E. et al., 1998. Ocean color chlorophyll algorithms for SeaWiFS. *Journal of Geophysical Research* 103, 24,937–24,954.
- O'Reilly, J.E. et al., 2000. Ocean color chlorophyll-a algorithms for SeaWiFS, Oc2 and Oc4: version 4. In: Hooker, S.B., Firestone, E.R. (Eds.), *SeaWiFS Postlaunch Technical Report Series*. NASA Goddard Space Flight Center, Greenbelt (MD, USA), pp. 9–23.
- Otero, M.P., Siegel, D., 2004. Spatial and temporal characteristics of sediment plumes and phytoplankton blooms in the Santa Barbara channel. *Deep-Sea Research II* 51, 1129–1149.
- Pan, X.J. et al., 2012. Remote sensing of phytoplankton community composition along the northeast coast of the United States. *Remote Sensing of Environment* 115, 3731–3747.
- Pan, X. et al., 2013. Remote sensing of picophytoplankton distribution in the Northern South China Sea. *Remote Sensing of Environment* 128, 162–175.
- Park, J. et al., 2010a. Variability of SeaWiFS chlorophyll-a in the southwest Atlantic sector of the southern ocean: strong topographic effects and weak seasonality. *Deep Sea Research Part I: Oceanographic Research Papers* 57, 604–620.
- Park, Y.J. et al., 2010b. Detection of algal blooms in European waters based on satellite chlorophyll data from MERIS and MODIS. *International Journal of Remote Sensing* 31, 6567–6583.
- Peñafiel, E.L. et al., 2007. Detection of monsoonal phytoplankton blooms in Luzon Strait with MODIS data. *Remote Sensing of Environment* 109, 443–450.
- Platt, T., Sathyendranath, S., 1999. Spatial structure of pelagic ecosystem processes in the global ocean. *Ecosystems* 2, 384–394.
- Platt, T., Sathyendranath, S., 2008. Ecological indicators for the pelagic zone of the ocean from remote sensing. *Remote Sensing of Environment*.
- Platt, T. et al., 2008. Operational estimation of primary production at large geographical scales. *Remote Sensing of Environment* 112, 3437–3448.
- Platt, T. et al., 2009. The phenology of phytoplankton blooms: ecosystem indicators from remote sensing. *Ecological Modelling* 220, 3057–3069.
- Qin, Y. et al., 2007. Validity of SeaDAS water constituents retrieval algorithms in Australian tropical coastal waters. *Geophysical Research Letters*, 34.
- Quarly, G.D., Srokosz, M.A., 2004. Eddies in the southern Mozambique Channel. *Deep Sea Research Part II: Topical Studies in Oceanography* 51 (1–3), 69–83.
- Racault, M.-F. et al., 2012. Phytoplankton phenology in the global ocean. *Ecological Indicators* 14, 152–163.
- Radenac, M.-H. et al., 2013. A very oligotrophic zone observed from space in the equatorial Pacific warm pool. *Remote Sensing of Environment* 134, 224–233.
- Raittis, D.E. et al., 2011. Assessing chlorophyll variability in relation to the environmental regime in Pagasitikos Gulf, Greece. *Journal of Marine Systems* 94, 16–22.
- Raj, R.P. et al., 2010. Oceanic and atmospheric influences on the variability of phytoplankton bloom in the Southwestern Indian Ocean. *Journal of Marine Systems* 82, 217–229.
- Richardson, L.L., 1996. Remote sensing of algal bloom dynamics. *Bioscience* 46, 492–501.
- Richardson, K., 1997. Harmful or exceptional phytoplankton blooms in the marine ecosystem. *Advances in Marine Biology* 31, 301–385.
- Richardson, A.J., Schoemann, D.S., 2004. Climate impact on plankton ecosystems in the Northeast Atlantic. *Science* 305, 1609–1612.
- Robinson, I.S., 2004. *Measuring the Oceans from Space: The Principle and Methods of Satellite Oceanography*. Springer – Praxis, Chichester, UK.
- Robinson, C.L.K. et al., 2004. Twenty years of satellite observations describing phytoplankton blooms in seas adjacent to GwaiiHaanas National Park Reserve, Canada. *Canadian Journal of Remote Sensing* 30, 36–43.
- Ruddick, K.G. et al., 2001. Optical remote sensing of chlorophyll a in case 2 waters by use of an adaptive two-band algorithm with optimal error properties. *Applied Optics* 40, 3575–3585.
- Ruddick, K. et al., 2008. Overview of ocean colour: theoretical background, sensors and applicability to detection and monitoring of harmful algal blooms (capabilities and limitations). In: Babin, M. et al. (Eds.), *Real-Time Coastal Observing Systems for Marine Ecosystem Dynamics and Harmful Algal Blooms*. UNESCO Publishing, pp. 331–383.
- Ryan, J.P. et al., 2008. A coastal ocean extreme bloom incubator. *Geophysical Research Letters* 35, L12602.
- Ryan, J.P. et al., 2009. Influences of upwelling and downwelling winds on red tide bloom dynamics in Monterey Bay, California. *Continental Shelf Research* 29, 785–795.
- Saitoh, S.-I. et al., 2002. A description of temporal and spatial variability in the Bering Sea spring phytoplankton blooms (1997–1999) using satellite multi-sensor remote sensing. *Progress in Oceanography* 55, 131–146.
- Santolieri, R. et al., 2003. Year-to-year variability of the phytoplankton bloom in the Southern Adriatic Sea (1998–2000): sea-viewing wide field-of-view sensor observations and modeling study. *Journal of Geophysical Research* 108, 8122.
- Sasamal, S.K. et al., 2005. Asterionella blooms in the Northwestern Bay of Bengal during 2004. *International Journal of Remote Sensing* 26, 3853–3858.
- Sathyendranath, S. et al., 2001. Remote sensing of phytoplankton pigments: a comparison of empirical and theoretical approach. *International Journal of Remote Sensing* 22, 249–273.
- Sathyendranath, S. et al., 2004. Discrimination of diatoms from other phytoplankton using ocean color data. *Marine Ecology Progress Series* 272, 59–68.
- Scargle, J.D., 1982. Studies in astronomical time series analysis. II. Statistical aspects of unevenly spaced data. *Astrophysical Journal*, 757–763.
- Sen Gupta, A., McNeil, B., 2012. Variability and change in the ocean. In: Henderson-Sellers, A., McGuffie, K. (Eds.), *The Future of the World's Climate*, second ed. Elsevier, Boston, pp. 141–165.
- Shang, S. et al., 2010. MODIS observed phytoplankton dynamics in the Taiwan Strait: an absorption-based analysis. *Biogeosciences Discussions* 7, 7795–7819.
- Shanmugam, P., 2011. A new bio-optical algorithm for the remote sensing of algal blooms in complex ocean waters. *Journal of Geophysical Research-Oceans* 116, 12.
- Shanmugam, P. et al., 2008. SeaWiFS sensing of hazardous algal blooms and their underlying mechanisms in shelf-slope waters of the Northwest Pacific during summer. *Remote Sensing of Environment* 112, 3248–3270.
- Shen, L. et al., 2012. Satellite remote sensing of harmful algal blooms (HAB) and a potential synthesized framework. *Sensors* 12, 7778–7803.
- Shevyrnogov, A. et al., 2002a. Spatial and temporal anomalies of chlorophyll concentration in Atlantic Ocean (by space-based data). *Advances in Space Research* 30, 2541–2546.
- Shevyrnogov, A. et al., 2002b. Trends of chlorophyll concentration in the surface layer of the northern and central Atlantic, a satellite data-based study. *Advances in Space Research* 30, 2535–2540.
- Shi, W., Wang, M., 2007. Observations of a Hurricane Katrina-induced phytoplankton bloom in the Gulf of Mexico. *Geophysical Research Letters*, 34.
- Shutler, J.D. et al., 2010. Coccolithophore bloom detection in the north east Atlantic using SeaWiFS: algorithm description, application and sensitivity analysis. *Remote Sensing of Environment* 114, 1008–1016.
- Shutler, J.D. et al., 2012. An adaptive approach to detect high-biomass algal blooms from EO chlorophyll-a data in support of harmful algal bloom monitoring. *Remote Sensing Letters* 3, 101–110.
- Siegel, H. et al., 1999. Case studies on phytoplankton blooms in coastal and open waters of the Baltic Sea using coastal zone color scanner data. *International Journal of Remote Sensing* 20, 1249–1264.
- Siegel, D.A. et al., 2002. The North Atlantic spring phytoplankton bloom and Sverdrup's critical depth hypothesis. *Science* 296, 730–733.
- Siegel, H. et al., 2007. Identification of coccolithophore blooms in the SE Atlantic Ocean off Namibia by satellites and in-situ methods. *Continental Shelf Research* 27, 258–274.
- Siegel, D.A. et al., 2013. Regional to Global assessments of phytoplankton dynamics from the SeaWiFS mission. *Remote Sensing of Environment* 135, 77–91.
- Signorini, S.R., McClain, C.R., 2009. Environmental factors controlling the Barents Sea spring–summer phytoplankton blooms. *Geophysical Research Letters* 36, L10604.
- Siswanto, E. et al., 2013. Detection of harmful algal blooms of Karenia mikimotoi using MODIS measurements: a case study of Seto-Inland Sea, Japan. *Remote Sensing of Environment* 129, 185–196.
- Smetacek, V., Cloern, J.E., 2008. On phytoplankton trends: how are phytoplankton at coastal sites around the world responding to ongoing global change? *Science* 319, 1346–1348.
- Song, H. et al., 2010. Phenology of phytoplankton blooms in the Nova Scotian shelf-Gulf of Maine region: remote sensing and modeling analysis. *Journal of Plankton Research* 32, 1485–1499.
- Sournia, A. et al., 1991. Marine phytoplankton: how many species in the world ocean? *Journal of Plankton Research* 13, 1093–1099.
- Srokosz, M.A., Quarly, G.D., 2013. The Madagascar Bloom – a serendipitous study. *Journal of Geophysical Research* 118 (1), 14–25.
- Srokosz, M.A., Quarly, G.D., Buck, J.J.H., 2004. A possible plankton wave in the Indian Ocean. *Geophysical Research Letters* 31 (13), L13301.
- SteemannNielsen, E., 1937. The Annual Amount of Organic Matter Produced by the Phytoplankton in the Sound off Helsingør. *MeddelelserfraKommisionen for DanmarksFiskeriogHavundersogelser*. Ser. Plankton, pp. 1–37.
- Steemann Nielsen, E., 1963. *Productivity, definition and measurement*. In: Hill, M.N. (Ed.), *The Sea*. Wiley, London.
- Steemann Nielsen, E., Jensen, E., 1957. Primary Ocean Production. The Autotrophic Production of Organic Matter in the Oceans. *Galathea Report*, pp. 49–136.
- Stumpf, R.P., 2001. Applications of satellite ocean color sensors for monitoring and predicting harmful algal blooms. *Human and Ecological Risk Assessment* 7, 1363–1368.
- Stumpf, R.P. et al., 2003. Monitoring Karenia brevis blooms in the Gulf of Mexico using satellite ocean color imagery and other data. *Harmful Algae* 2, 147–160.
- Subramaniam, A., Carpenter, E.J., 1994. An empirically derived protocol for the detection of blooms of the marine cyanobacteria *Trichodesmium* using CZCS imagery. *International Journal of Remote Sensing* 15, 1559–1569.
- Subramaniam, A. et al., 1999a. Bio-optical properties of the marine diazotrophic cyanobacteria *Trichodesmium* spp.; II. A reflectance model for remote-sensing. *Limnology and Oceanography* 44, 618–627.
- Subramaniam, A. et al., 1999b. Bio-optical properties of the marine diazotrophic cyanobacteria *Trichodesmium* spp.; I. Absorption and photosynthetic action spectra. *Limnology and Oceanography* 44, 608–617.

- Subramaniam, A. et al., 2002. Detecting *Trichodesmium* blooms in SeaWiFS imagery. Deep-Sea Research II 49, 107–121.
- Tan, C.K. et al., 2006. Seasonal variability of SeaWiFS chlorophyll a in the Malacca Straits in relation to Asian monsoon. Continental Shelf Research 26, 168–178.
- Tang, D.-L. et al., 1999. Remote sensing observations of winter phytoplankton blooms southwest of the Luzon Strait in the South China Sea. Marine Ecology Progress Series 191, 45–51.
- Tang, D.L. et al., 2004. Long-time observation of annual variation of Taiwan Strait upwelling in summer season. Advances in Space Research 33, 307–312.
- Tang, D. et al., 2006. Satellite evidence of harmful algal blooms and related oceanographic features in the Bohai Sea during Autumn 1998. Advances in Space Research 37, 681–689.
- Thomas, A.C. et al., 2003. Satellite-measured phytoplankton variability in the Gulf of Maine. Continental Shelf Research 23, 971–989.
- Thomas, A.C. et al., 2012. Satellite views of Pacific chlorophyll variability: comparisons to physical variability, local versus nonlocal influences and links to climate indices. Deep Sea Research Part II: Topical Studies in Oceanography, 10.
- Tilstone, G. et al., 2011a. Variability in specific-absorption properties and their use in a semi-analytical ocean colour algorithm for MERIS in North Sea and Western English Channel coastal waters. Remote Sensing of Environment 118, 320–338.
- Tilstone, G.H. et al., 2011b. An assessment of chlorophyll-a algorithms available for SeaWiFS in coastal and open areas of the Bay of Bengal and Arabian Sea. Remote Sensing of Environment.
- Tiwari, S.P., Shamugam, P., 2013. Evaluation of inversion models for the satellite retrieval of absorption coefficient of phytoplankton in oceanic/coastal waters. IEEE Journal of Selected Topics in Applied Earth Observations and Remote Sensing, 99.
- Tomlinson, M.C. et al., 2004. Evaluation of the use of SeaWiFS imagery for detecting *Karenia brevis* harmful algal blooms in the Eastern Gulf of Mexico. Remote Sensing of Environment 91, 293–303.
- Tomlinson, M.C. et al., 2008. An evaluation of remote sensing techniques for enhanced detection of the toxic dinoflagellate, *Karenia brevis*. Remote Sensing of Environment 113, 598–609.
- Torrecilla, E. et al., 2011. Cluster analysis of hyperspectral optical data for discriminating phytoplankton pigment assemblages in the open ocean. Remote Sensing of Environment 115, 2578–2593.
- Tyrell, T. et al., 2005. Effect of seafloor depth on phytoplankton blooms in high-nitrate, low-chlorophyll (HNLC) regions. Journal of Geophysical Research, 110.
- Uiboupin, R. et al., 2012. Monitoring the effect of upwelling on the chlorophyll a distribution in the Gulf of Finland (Baltic Sea) using remote sensing and in situ data. Oceanologia 54, 395–419.
- Uitz, J. et al., 2006. From surface chlorophyll a to phytoplankton community composition in oceanic waters. Journal of Geophysical Research, 111.
- Urquhart, E.A. et al., 2013. Geospatial interpolation of MODIS-derived salinity and temperature in the Chesapeake Bay. Remote Sensing of Environment 135, 167–177.
- Uz, B.M., 2007. What causes the sporadic phytoplankton bloom Southeast of Madagascar? Journal of Geophysical Research (Oceans) 112, C09010.
- Vargas, M. et al., 2009. Phenology of marine phytoplankton from satellite ocean color measurements. Geophysical Research Letters, 36.
- Venables, H.J. et al., 2007. Physical conditions controlling the development of a regular phytoplankton bloom North of the Crozet Plateau, Southern Ocean. Deep Sea Research Part II: Topical Studies in Oceanography 54, 1949–1965.
- Villareal, T.A., Adornato, L., Wilson, C., Schoenbaechler, C.A., 2011. Summer blooms of diatom-diazotroph assemblages and surface chlorophyll in the North Pacific gyre: a disconnect. Journal of Geophysical Research 116 (C3), C03001.
- Villareal, T.A. et al., 2012. Summer diatom blooms in the North Pacific Subtropical Gyre: 2008–2009. PLoS One 7, e33109.
- Vinayachandran, P.N., Mathew, S., 2003. Phytoplankton bloom in the Bay of Bengal during the northeast monsoon and its intensification by cyclones. Geophysical Research Letters 30, 1572.
- Volpe, G. et al., 2007. The colour of the Mediterranean Sea: global versus regional bio-optical algorithms evaluation and implication for satellite chlorophyll estimates. Remote Sensing of Environment 107, 625–638.
- Voss, K.J. et al., 1998. Scattering and attenuation properties of *Emiliania huxleyi* cells and their detached coccoliths. Limnology and Oceanography 43, 870–876.
- Wan, Z. et al., 2013. Comparison of two light attenuation parameterization focusing on timing of spring bloom and primary production in the Baltic Sea. Ecological Modelling 259, 40–49.
- Wang, D., Zhao, H., 2008. Estimation of phytoplankton responses to Hurricane Gonu over the Arabian Sea based on ocean color data. Sensors 8, 4878–4893.
- Wang, J. et al., 2010. Winter phytoplankton bloom induced by subsurface upwelling and mixed layer entrainment southwest of Luzon Strait. Journal of Marine Systems 83, 141–149.
- Westberry, T.K. et al., 2005. An improved bio-optical model for the remote sensing of *Trichodesmium* spp. blooms. Journal of Geophysical Research 110 (C06012), 1–11.
- Westberry, T.K. et al., 2013. Retrospective satellite ocean color analysis of purposeful and natural ocean iron fertilization. Deep Sea Research Part I: Oceanographic Research Papers 73, 1–16.
- White, A.E. et al., 2007. What factors are driving summer phytoplankton blooms in the North Pacific Subtropical Gyre? Journal of Geophysical Research (Oceans), 112.
- Wilson, C., 2003. Late summer chlorophyll blooms in the oligotrophic North Pacific Subtropical Gyre. Geophysical Research Letters 30 (18).
- Wilson, C., 2011. The rocky road from research to operations for satellite ocean-colour data in fishery management. ICES Journal of Marine Science 68, 677–686.
- Wilson, C., Qiu, X., 2008. Global distribution of summer chlorophyll blooms in the oligotrophic gyres. Progress in Oceanography 78 (2), 107–134.
- Wilson, C., Villareal, T.A., Maximenko, N., Bograd, S.J., Montoya, J.P., Schoenbaechler, C.A., 2008. Biological and physical forcings of late summer chlorophyll blooms at 30°N in the oligotrophic Pacific. Journal of Marine Systems 69 (3–4), 164–176.
- Wong, K.T.M. et al., 2009. Forecasting of environmental risk maps of coastal algal blooms. Harmful Algae 8, 407–420.
- Xing, X.-G. et al., 2007. An overview of remote sensing of chlorophyll fluorescence. Ocean Science Journal 42, 49–59.
- Yentsch, C.S., Menzel, D.W., 1963. A method for the determination of phytoplankton chlorophyll and phaeophytin by fluorescence. Deep Sea Research and Oceanographic Abstracts 10, 221–231.
- Yoder, J.A. et al., 2001. Variability in coastal zone color scanner (CZCS) chlorophyll imagery of ocean margin waters off the US east coast. Continental Shelf Research 21, 1191–1218.
- Yoo, S. et al., 2008. Seasonal, interannual and event scale variation in North Pacific ecosystems. Progress in Oceanography 77, 155–181.
- Yuan, J. et al., 2005. In-pixel variations of chl a fluorescence in the Northern Gulf of Mexico and their implications for calibrating remotely sensed chl a and other products. Continental Shelf Research 25, 1894–1904.
- Zeichen, M.M., Robinson, I.S., 2004. Detection and monitoring of algal blooms using SeaWiFS imagery. International Journal of Remote Sensing 25, 1389–1395.
- Zhao, H. et al., 2008. Comparison of phytoplankton blooms triggered by two typhoons with different intensities and translation speeds in the South China Sea. Marine Ecology Progress Series 365, 57–65.
- Zhao, H. et al., 2009a. Phytoplankton Blooms near the Pearl River estuary induced by Typhoon Nuri. Journal of Geophysical Research 114 (12).
- Zhao, J. et al., 2009b. The variations in optical properties of CDOM throughout an algal bloom event. Estuarine, Coastal and Shelf Science 82, 225–232.
- Zhao, D. et al., 2010. The relation of chlorophyll-a concentration with the reflectance peak near 700 nm in algae-dominated waters and sensitivity of fluorescence algorithms for detecting algal bloom. International Journal of Remote Sensing 31 (10).
- Zhong, Y., Bracco, A., Villareal, T.A., 2012. Pattern formation at the ocean surface: *Sargassum* distribution and the role of the eddy field. Limnology and Oceanography: Fluids & Environments 2, 12–27. <http://dx.doi.org/10.1215/21573689-1573372>.
- Zingone, A. et al., 2010. Multiscale variability of twenty-two coastal phytoplankton time series: a global scale comparison. Estuaries and Coasts 33, 224–229.